Progress in Fractional Differentiation and Applications
An International Journal

http://dx.doi.org/10.18576/pfda/110113

Laplace Fractional Residual Power Series Scheme for Caputo Time-Schrodinger Fractional Equations

Hussam Aljarrah[1], *Mohammad Alaroud*[2], *Anuar Ishak*[1], *Maslina Darus*[1] , *Shrideh Al-Omari*[3,*] *and Mona Khandaqji* [4]

[1] Department of Mathematical Sciences, Faculty of Science and Technology, Universiti Kebangsaan Malaysia (UKM), Bangi 43600, Selangor, Malaysia
[2] Department of Mathematics, Faculty of Arts and Science, Amman Arab University, Amman 11953, Jordan
[3] Department of Mathematics, Faculty of Science, Al-Balqa Applied University, Salt 11134, Jordan
[4] Department of Basic Science, Faculty of Arts and Science, Applied Science Private University, Amman 11931, Jordan

Received: 3 Jun. 2024, Revised: 12 Jul. 2024, Accepted: 2 Sep. 2024
Published online: 1 Jan. 2025

Abstract: The time-fractional Schrodinger equations (FSEs) have various applications in quantum mechanics and physical sciences as they describe a wide range of wave propagation phenomena including dust-acoustic, Langmuir and electromagnetic waves in the plasma physics. This article aims to employ the Laplace fractional residual power series (RPS) scheme to derive exact and approximate solutions for the FSEs in a time-Caputo sense following a limit concept. By employing the aforementioned Laplace fractional residual power series method, we establish complex linear and complex nonlinear fractional order models and evaluate efficacy of such a method by conducting numerical experiments as an application. Throughout the furnished computations, we include a comparison between the approximate values and their corresponding exact solutions and obtain some analysis on the absolute error. Moreover, 2D and 3D-graphical representations are introduced to display depiction of the dynamic behaviour of the attained solutions in a specific domain. Further, we confirm reliability of solutions generated by the method of the suggested scheme by comparing them with previously established solutions. Such comparisons are shown to be harmonic with the compared methods, which confirms that the Laplace fractional residual power series approach is an alternative, straightforward, precise and effective for solving both linear and non-linear partial differential equations of fractional order. Moreover, we provide numerical and graphical forms to validate the approach.

Keywords: Time-fractional Schrodinger equations, Laplace transform, Laplace fractional residual power series, time-Caputo fractional derivative.

1 Introduction

The fractional calculus has witnessed a rapid growing attention by scientists due to its superb and distinguished characteristics. The fractional calculus has, consequently, been considered as a convenient tool for modelling and describing numerous complex fractional problems in varied and prevalent subjects of engineering and science including chemistry, physics, biology, ecology, mechanics, electrical engineering, medicine etc. [1-5]. From a modelling viewpoint, the fractional derivative is a powerful instrument which has been applied by scientists and analysts for simulating and interpreting sophisticated systems of non-linear dynamical processes. The main causes behind this follows from the fact that the order of derivative could be chosen arbitrary and the fractional derivative may characterize the memory and hereditary features of varied processes and materials on the past and present situations. Recently, diverse issues have been introduced to define the fractional derivative concept. The most frequently utilized definitions are the Atangana–Baleanu, Caputo–Fabrizio, Riemann– Liouville and Caputo issues. Although, the Caputo's fractional derivative remains the most preferred by researchers as it can precisely depict physically and practically the phenomena with the past memory [6-9]. Fractional partial differential equations (FPDEs) have a notable role in designing the dynamic behaviours of computational fractional models, which have riveted experts' interest to concentrate on its enormous applications in distinct scientific fields including diffusion processes, viscoelastic damping, fluid flow, quantum mechanics, heat transfer, kinetic theory, etc. [10-20]. The mathematical potent modelling of fractional models

* Corresponding author e-mail: mohmdnh@bau.edu.jo

containing complex-valued functions is a challenging task for scholars. Nevertheless, finding the closed-form and the analytical solutions to these models is intractable and hopeless in several circumstances. As a result, there is an insistent requirement to dependable numeric-analytic techniques. Further, well-known methods such as Homotopy analysis method, Adomian decomposition method, differential transform method, reproducing kernel method, variational iteration method and fractional residual power series method and so on [21-28]. The fractional RPS method is a semi-analytic technique used to solve differential equations that cannot be solved using other common methods like separation of variables or integrating factors. In this method, the solution is expressed as a power series and the coefficients of the series are calculated by using the recurrence relations derived from the differential equation. The general solution is obtained by combining the power series with the initial conditions. The method is called "residual" as it calculates the "residual", which is the difference between the left-hand side and the right-hand side of the equation. This residual is then used to calculate the coefficients of the power series. Many researchers have recently focused on the fractional RPS approach, which has successfully investigated a variety of FPDEs [29-33]. Although the method is a bit more involved than some other methods, where it is based on $(n-1)$-times FD of the residual-error function in each step and can be useful for solving a wide range of FDEs and FPDEs that cannot be solved by other means. So, this solution methodology is somewhat difficult for non-linear terms of certain classes of FPDEs. In order to avoid this intractably, the authors in [34] proposed a novel attractive technique that combines between the LT operator and the fractional RPS algorithm, namely the Laplace RPS algorithm. This novel method can generate fractional power series expansion (FPSE) solutions for both linear and non-linear FPDEs which do not require any physical restriction [35]. It also depends on the limit concept with minimal computations to find the specified coefficients [36-40]. Unlike the fractional RPS algorithm, which requires a multiple computations to calculate various FDs in the solution steps. As a result, by incorporating a fast convergence series, this proposed method can produce closed-form solutions as well as accurate approximate solutions.

The fractional Schrodinger equation is a generalization of the classical SE that includes time-FDs [41]. It has been used to model a wide range of physical phenomena, from anomalous diffusion in complex systems to the behavior of quantum particles in disordered media. The classical SE is a PDE that describes the evolution of a quantum state over time. It is written as [42]

$$i\mathrm{h}\frac{\partial}{\partial t}\mathscr{U} = H[\mathscr{U}],$$

where i is the imaginary unit, h is the reduced Planck constant, $\mathscr{U}$ is the wave function, t is time, and H is the Hamiltonian operator. The Hamiltonian operator is a mathematical operator that describes the total energy of a system. FSE is obtained by replacing the time-derivative in the classical SE with a time-FD of order a. The resulting equation is [43-45]

$$i\mathrm{h}\mathscr{D}_t^a\mathscr{U} = H[\mathscr{U}],$$

where $\mathscr{D}_t^a$ is the time-FD .

One of the most interesting properties of the FSE is its non-locality in time. The FD operator depends on the fact that the behavior of a system at a given time depends not only on its immediate past, but also on its history. This makes the equation particularly well-suited for modeling systems that exhibit long-range correlations in time as the anomalous diffusion in complex systems. Another interesting property of the FSE is its self-similarity. This means that the equation is invariant under rescaling of the space and time variables. This property has important consequences for the behavior of the solutions of the equation, which can exhibit fractal-like patterns [46-48]. FSE has been used to model a tremendous range of physical phenomena. One of the most important applications is in the study of anomalous diffusion in complex systems. Anomalous diffusion refers to the behavior of particles that do not follow the usual random walk behavior observed in simple systems. Instead, these particles exhibit long-range correlations in time, which can be captured by the FD operator in the FSE [49-52]. As well as, the FSE has been applied in the study of quantum particles in disordered media. In these systems, the Hamiltonian operator is not translationally invariant, which can lead to complex behavior of the quantum state. The FD operator in the FSE can capture the non-local effects of disorder on the quantum state [53 - 58].

In literature, numerous numerical and analytical methods have been discussed for studying the analytical and exact solutions of the time-FSEs [59]. These techniques have examined the time-FSEs in the meaning of R-L and Caputo FDs. But each of the mentioned approaches needs a lot of computational effort and long processing times, and also has its physical limitations. The novelty of the present work is to consider the Laplace fractional RPS algorithm in investigating the analytical and closed form solutions for the time-FSEs with an appropriate ICs in view of the time-Caputo-FD. Here, we have been selecting this type of FDs operator because of its harmonization with the ICs in treating wide range of FPDEs. The proposed method's accuracy and effectiveness have been confirmed through an absolute error interpretation of the studied problems. Additionally, numerical results obtained using the recommended algorithm have been compared with other techniques in terms of absolute errors. The results demonstrate excellent agreement with those of various other methods, highlighting the proposed approach's reliability and efficiency [60-67].

The remainder of the current article is structured as follows. A quick overview of the time-Caputo-FD concept and essential results relating to the LT and Laplace fractional RPS algorithm are given in Section 2. The methodology of performing the recommended approach for solving non-linear time-FSEs is drawn in Section 3. In Section 4, four applications of time-FSEs are stated to illustrate the accuracy and applicability of our approach. Graphical and numerical results are discussed and summarized in Section 5. Finally, the conclusion part is given in Section 6 .

2 Essential Concepts

This section provides an overview of the time-FD in a Caputo sense. It also includes a preliminary definitions and essential theorems concerning the LT and Laplace fractional RPS algorithm, which will be utilized in the subsequent sections. Understanding the concepts and principles of fractional differentiation is crucial for comprehending the upcoming discussions. Whereas, familiarity with the relevant definitions and theorems of the LT will be advantageous for subsequent analyses and interpretations.

Definition 1. The time–FD of the Caputo sense for $\mathscr{U}(x,t)$ of order a is defined by [3]

$$\mathfrak{D}_t^a \mathscr{U}(x,t) = \begin{cases} \mathscr{I}_t^{n-a}\left(D_t^n \mathscr{U}(x,t)\right), & 0 < n-1 < a \le n, \\ D_t^n \mathscr{U}(x,t), & a = n, \end{cases}$$

where $D_t^n = \frac{\partial^n}{\partial t^n}$, *and* $\mathscr{I}_t$ is the R-L integral operator of $\mathscr{U}(x,t)$.

Definition 2. Let $\mathscr{U}(x,t)$ be a piecewise continuous function of exponential order δ on $I \times [0\,,\infty)$, then the LT of $\mathscr{U}(x,t)$ is defined by [2]

$$U(x,s) = L[\mathscr{U}(x,t)] \int_0^\infty e^{-\mathfrak{s}t}\mathscr{U}(x,t)\,dt, \quad s > \delta.$$

The inverse LT of $\mathfrak{U}(x,\mathfrak{s})$ is defined by

$$\mathscr{U}(x,t) = \mathscr{L}^{-1}[\mathfrak{U}(x,\mathfrak{s})] = \int_{c-i\infty}^{c+i\infty} e^{\mathfrak{s}t}\mathfrak{U}(x,\mathfrak{s})\,d\mathfrak{s}, \quad c = Re(\mathfrak{s}) > \delta_0,.$$

Lemma 1. For two piecewise continuous functions $\mathscr{U}(x,t)$ and $\mathscr{V}(x,t)$, $I\times[0\,,\infty)$, of exponential orders δ_1 and δ_2, respectively, where $\delta_1 < \delta_2$, we have [2]

1. $\mathscr{L}[a\mathscr{U}(x,t) + b\mathscr{V}(x,t)] = a\mathfrak{U}(x,\mathfrak{s}) + b\bigvee(x,\mathfrak{s}), x \in I,\ \mathfrak{s} > \delta_1.$
2. $\mathscr{L}^{-1}[a\mathfrak{U}(x,\mathfrak{s}) + b\bigvee(x,\mathfrak{s})] = a\mathscr{U}(x,t) + b\mathscr{V}(x,t), x \in I,\ t \ge 0.$
3. $\mathscr{L}[e^{at}\mathscr{U}(x,t)] = \mathfrak{U}(x,\mathfrak{s}-a), x \in I,\ \mathfrak{s} > a + \delta_1.$
4. $lim_{\mathfrak{s}\to\infty}\,\mathfrak{s}\,\mathfrak{U}(x,\mathfrak{s}) = \mathscr{U}(x,0),\ x \in I.$
5. $\mathscr{L}[\mathfrak{D}_t^a\mathscr{U}(x,t)\,] = \mathfrak{s}^a\mathfrak{U}(x,\mathfrak{s}) - \sum_{k=0}^{n-1}\mathfrak{s}^{a-k-1}D_t^k\mathscr{U}(x,0)$, for $a \in (n-1,n]$,
6. $\mathscr{L}\left[\mathfrak{D}_t^{ja}\mathscr{U}(x,t)\,\right] = \mathfrak{s}^{ja}\mathfrak{U}(x,\mathfrak{s}) - \sum_{k=0}^{j-1}\mathfrak{s}^{(j-k)a-1}D_t^{ka}\mathscr{U}(x,0)$, for $a \in (0,1]$,

where $\mathfrak{U}(x,\mathfrak{s}) = \mathscr{L}[\mathscr{U}(x,t)]$, $\bigvee(x,\mathfrak{s}) = \mathscr{L}[\mathscr{V}(x,t)]$, and $a,b \in \mathbb{R}$.

Theorem 1. Let the Laplace fractional expansion (LFE) for the new function $\mathscr{U}(x,t)$, $\mathfrak{U}(x,\mathfrak{s}) = \mathscr{L}[\mathscr{U}(x,t)]$, is given by [2]

$$\mathfrak{U}(x,\mathfrak{s}) = \sum_{n=0}^{\infty}\frac{h_n(x)}{\mathfrak{s}^{na+1}},\ x \in I,\ \mathfrak{s} > \delta,\ 0 < a \le 1,$$

then $h_n(x) = \mathfrak{D}_t^{na}\mathscr{U}(x,0)$.

Theorem 2. Suppose that the transformation function $\mathfrak{U}(x,\mathfrak{s})$ can be formulated as in Theorem 1. Then, for all $(x,\mathfrak{s}) \in I\times(\delta\,,\gamma]$, and $a \in (0,1]$ such that $\left|\mathfrak{s}\mathscr{L}\left[\mathfrak{D}_t^{(n+1)a}\mathscr{U}(x,\mathfrak{s})\,\right]\right| \le g$, the reminder R_n of the new Laplace expansion fulfills the following inequality [2]

$$|R_n(x,\mathfrak{s})| \le \frac{M(x)}{\mathfrak{s}^{1+(n+1)a}},\ x \in I,\ \delta < \mathfrak{s} \le \gamma,$$

where $M(x)$ is a function of x.

3 Principle of Laplace fractional RPS technique for the non-linear time-FSEs

The Laplace fractional RPS scheme is a novel analytical technique proved in [34] to handle complicated non-linear time-FPDEs arising in various disciplines in natural science and engineering. This section highlights the steps of the Laplace fractional RPS solution for the considered problem. The first step in this method is to transform the targeted equation to the Laplace space and discover the algebraic solution (LFE) of the transformed equation in a new space, where the resultant series coefficients is found via a limit concept. Finally, we find the inverse LT for the previously obtained solution into its original space and hence, the problem can be solved. To perform the solution methodology of our scheme, let us consider the following form of the non-linear time-FSE with IC's

$$\begin{cases} i\mathfrak{D}_t^a \mathscr{U}(,t) = H[\mathscr{U}(,t)],\ 0<a\leq 1, \\ \text{subject to IC}'\text{s}: \\ \mathscr{U}(,0) = \mathscr{P}_j(),\ j=1,2,\ldots,n \end{cases} \tag{1}$$

Subsequent, the guidelines for generating the approximate solution for Equation 1 by the Laplace fractional RPS algorithm are summarized in the following six steps:

1- We apply the LT to both sides of (1) with the IC's of (1), relying on Lemma 1, to have

$$\mathfrak{U}(,\mathfrak{s}) = \frac{\mathscr{P}_j()}{\mathfrak{s}} + \frac{i}{\mathfrak{s}^a}\left(\mathscr{L}\{H[\mathscr{U}(,t)]\}\right), \tag{2}$$

where $\mathfrak{U}(,\mathfrak{s}) = \mathscr{L}[\mathscr{U}(,t)](\mathfrak{s})$, $\mathfrak{s}>\delta$.

2- We assume that the approximate solution of the Laplace equation (2) has the following LFE based on Theorem 1,

$$\mathfrak{U}(,\mathfrak{s}) = \frac{\mathscr{P}_j()}{\mathfrak{s}} - i\sum_{n=1}^{\infty}\frac{h_n()}{\mathfrak{s}^{na+1}},\ \in\overline{I},\ \mathfrak{s}>\delta\geq 0, \tag{3}$$

and the $k-th$ LFE series solution is written as

$$\mathfrak{U}_k(,\mathfrak{s}) = \frac{\mathscr{P}_j()}{\mathfrak{s}} - i\sum_{n=1}^{k}\frac{h_n()}{\mathfrak{s}^{na+1}},\ \in\overline{I},\ \mathfrak{s}>\delta\geq 0\,. \tag{4}$$

3- The $k-th$ Laplace fractional residual-error (LFRE) function of (1) is identified as

$$\mathscr{L}\left(Res_{\mathfrak{U}_k}(,\mathfrak{s})\right) = \frac{\mathscr{P}_j()}{\mathfrak{s}} + \frac{i}{\mathfrak{s}^a}\left(\mathscr{L}\{H[\mathscr{U}(,t)]\}\right), \tag{5}$$

and the LFRE function of (1) is formulated as

$$\lim_{k\to\infty}\mathscr{L}\left(Res_{\mathfrak{U}_k}(,\mathfrak{s})\right) = \mathscr{L}\left(Res_{\mathfrak{U}}(,\mathfrak{s})\right) = \frac{\mathscr{P}_j()}{\mathfrak{s}} + \frac{i}{\mathfrak{s}^a}\left(\mathscr{L}\{H[\mathscr{U}(,t)]\}\right). \tag{6}$$

As in [34], some useful facts of the LFRE which are important in designing and building the approximate solution are mentioned below:

1. $lim_{k\to\infty}\mathscr{L}\left(Res_{\mathfrak{U}_k}(,\mathfrak{s})\right) = \mathscr{L}\left(Res_{\mathfrak{U}}(,\mathfrak{s})\right)$, for $\in\overline{I}$, $\mathfrak{s}>\delta\geq 0$.

2. $\mathscr{L}\left(Res_{\mathfrak{U}}(,\mathfrak{s})\right) = 0$, for $\in\overline{I}$, $\mathfrak{s}>\delta\geq 0$.

3. $\lim_{\mathfrak{s}\to\infty}\mathfrak{s}^{ka+1}\mathscr{L}\left(Res_{\mathfrak{U}_k}(,\mathfrak{s})\right) = 0$, for $\in\overline{I}$, $\mathfrak{s}>\delta\geq 0$, and $k=1,2,3,\ldots$.

4. We consider the $k-th$ LFE series solution (4) into the $k-th$ LFRE of (5).

5. We look for the solution of $\lim_{\mathfrak{s}\to\infty}\mathfrak{s}^{ka+1}\mathscr{L}\left(Res_{\mathfrak{U}_k}(,\mathfrak{s})\right) = 0$ to get the unknown coefficients $h_k()$, for $k=2,\ 3,\ 4\ldots$. These unknown variables are then accumulated in terms of the LFE series (4), $\mathfrak{U}_k(,\mathfrak{s})$.

6. The inverse LT operator can be used for both sides of the resulted LFE series solution to find the approximate solution $\mathscr{U}_k(,t)$ of the studied problem (1).

4 Numerical Applications

To elucidate the features, performance, and applicability of the Laplace fractional RPS algorithm, the different quantum mechanics applications consisting of both linear and non-linear time-FSEs with time- Caputo FDs are analytically and numerically shown. In this context, the accurate approximate solutions for four Schrödinger models in light of time-Caputo meaning are investigated at distinct FD values' utilizing the solution methodology of our recommended scheme. The generated solutions carried out with minimal computational work and provides the same exact solutions compared to well-known approaches [60-67]. It is worth mentioning that we have utilized MATHEMATICA 12 software package to implement all calculations and graphics.

Application 1. Consider the linear time-FSE in [60, 61, 65, 66]:

$$\mathscr{D}_t^a \mathscr{U} + i\mathscr{U}_{xx} = 0, \tag{7}$$

subjecttotheIC, $\mathscr{U}(x,0) = 1+\cosh(2x)$, where $a \in (0,1]$, $i^2 = -1$ and the complex function $\mathscr{U}(x,t) : \Omega \to \mathbb{C}$. The exact solutions when $a = 1$ is $\mathscr{U}(x,t) = 1+\cosh(2x)\, e^{-4it}$. Following the analysis presented above, we can obtain the Laplace fractional equation for (7) as

$$\mathfrak{U}(x,\mathfrak{s}) = \frac{1+\cosh(2x)}{\mathfrak{s}} - \frac{i}{\mathfrak{s}^a}\mathscr{L}\left\{\frac{\partial^2}{\partial x^2}\mathscr{L}^{-1}\{\mathfrak{U}\}\right\}, \tag{8}$$

where $\mathscr{L}[\mathscr{U}(x,t)] = \mathfrak{U}(x,\mathfrak{s})$. Also, according to the method discussion, the $k-th$-LFE series solution $\mathfrak{U}_k(x,\mathfrak{s})$ for (8) can be written as

$$\mathfrak{U}_k(x,\mathfrak{s}) = \frac{1+\cosh(2x)}{\mathfrak{s}} + \sum_{n=1}^{k} \frac{h_n(x)}{\mathfrak{s}^{na+1}}. \tag{9}$$

Next, based on the method, the $k-th$-truncated LFRE function of (8) can be identified as

$$\mathscr{L}\left(Res_{\mathfrak{U}_k}(x,\mathfrak{s})\right) = \sum_{n=1}^{k} \frac{h_n(x)}{\mathfrak{s}^{na+1}} + \frac{i}{\mathfrak{s}^a}\mathscr{L}\left\{\frac{\partial^2}{\partial x^2}\mathscr{L}^{-1}\{\mathfrak{U}_k\}\right\}. \tag{10}$$

To get the $1-st$ LFRE function we let $k = 1$ in (10), one can obtain that

$$\mathscr{L}\left(Res_{\mathfrak{U}_1}(x,\mathfrak{s})\right) = \frac{h_1(x)}{\mathfrak{s}^{a+1}} + \frac{i}{\mathfrak{s}^a}\mathscr{L}\left\{\frac{\partial^2}{\partial x^2}\mathscr{L}^{-1}\left\{\frac{1+\cosh(2x)}{\mathfrak{s}} + \frac{h_1(x)}{\mathfrak{s}^{a+1}}\right\}\right\} = \frac{h_1(x)+4i\cosh(2x)}{\mathfrak{s}^{a+1}} + \frac{ih_1''(x)}{\mathfrak{s}^{2a+1}}. \tag{11}$$

By performing the following process, $\lim_{\mathfrak{s}\to\infty} \mathfrak{s}^{a+1}\,\mathscr{L}\left(Res_{\mathfrak{U}_1}(x,\mathfrak{s})\right) = 0$, which gives us that $h_1(x) = -4i\cosh(2x)$. And so, the $1-st$ LFE series solution of (8) can be written as

$$\mathfrak{U}_1(x,\mathfrak{s}) = \frac{1+\cosh(2x)}{\mathfrak{s}} + \frac{(-4i)\cosh(2x)}{\mathfrak{s}^{a+1}}. \tag{12}$$

To get the $2-nd$ LFRE function we let $k = 2$ in (10), one can obtain that

$$\mathscr{L}\left(Res_{\mathfrak{U}_2}(x,\mathfrak{s})\right) = \frac{h_2(x) - (-4i)^2\cosh(2x)}{\mathfrak{s}^{2a+1}} + \frac{ih_2''(x)}{\mathfrak{s}^{3a+1}} \tag{13}$$

By performing the following process, $\lim_{\mathfrak{s}\to\infty} \mathfrak{s}^{2a+1}\,\mathscr{L}\left(Res_{\mathfrak{U}_2}(x,\mathfrak{s})\right) = 0$, we get that $h_2(x) = (-4i)^2\cosh(2x)$. And so, the $2-nd$ LFE series solution of (**??**) can be formulated as

$$\mathfrak{U}_3(x,\mathfrak{s}) = \frac{1+\cosh(2x)}{\mathfrak{s}} + \frac{(-4i)\cosh(2x)}{\mathfrak{s}^{a+1}} + \frac{(-4i)^2\cosh(2x)}{\mathfrak{s}^{2a+1}}. \tag{14}$$

The same matter for $k = 3$ reveals

$$\mathscr{L}\left(Res_{\mathfrak{U}_3}(x,\mathfrak{s})\right) = \frac{h_3(x) - (-4i)^3\cosh(2x)}{\mathfrak{s}^{3a+1}} + \frac{ih_3''(x) - (4i)^2\cosh(2x)}{\mathfrak{s}^{4a+1}}. \tag{15}$$

By solving $\lim_{\mathfrak{s}\to\infty}\mathfrak{s}^{3a+1}\,\mathscr{L}\left(Res_3\left(x,\mathfrak{s}\right)\right)=0$, we obtain that $h_3\left(x\right)=\left(-4i\right)^3\cosh\left(2x\right)$. Hence, the $3-rd$ Laplace series solution of (8) is

$$\mathfrak{U}_3\left(x,\mathfrak{s}\right)=\frac{1+\cosh\left(2x\right)}{\mathfrak{s}}+\frac{\left(-4i\right)\cosh\left(2x\right)}{\mathfrak{s}^{a+1}}+\frac{\left(-4i\right)^2\cosh\left(2x\right)}{\mathfrak{s}^{2a+1}}+\frac{\left(-4i\right)^3\cosh\left(2x\right)}{\mathfrak{s}^{3a+1}}. \tag{16}$$

In a similar way, the above process can be repeated smoothly using Mathematica for $k=4,5,6,\ldots$, and since $\lim_{\mathfrak{s}\to\infty}\mathfrak{s}^{ka+1}\,\mathscr{L}\left(Res_{\mathfrak{U}_k}\left(x,\mathfrak{s}\right)\right)=0$, one can obtain that $h_k\left(x\right)=\left(-4i\right)^k\cosh\left(2x\right)$.

Consequently, if we collect all the previous results, the $k-th$ truncated LFE series solution of (8) can be written in the shape

$$\begin{aligned}\mathfrak{U}_k\left(x,\mathfrak{s}\right)&=\frac{1+\cosh\left(2x\right)}{\mathfrak{s}}+\frac{\left(-4i\right)\cosh\left(2x\right)}{\mathfrak{s}^{a+1}}+\frac{\left(-4i\right)^2\cosh\left(2x\right)}{\mathfrak{s}^{2a+1}}+\frac{\left(-4i\right)^3\cosh\left(2x\right)}{\mathfrak{s}^{3a+1}}+\cdots+\frac{\left(-4i\right)^k\cosh\left(2x\right)}{\mathfrak{s}^{ka+1}}\\&=\frac{1}{\mathfrak{s}}+\cosh\left(2x\right)\left(\sum_{n=0}^{k}\frac{\left(-4i\right)^n}{\mathfrak{s}^{na+1}}\right).\end{aligned} \tag{17}$$

If we transform back expansion (17), one can rewrite the $k-th$ truncated approximate solution of (7) in the following expansion

$$\mathscr{U}_k\left(x,t\right)=1+\cosh\left(2x\right)\left(\sum_{n=0}^{k}\left(-4i\right)^n\frac{t^{na}}{\Gamma\left(na+1\right)}\right). \tag{18}$$

For the stander case $a=1$, the solution of (7) can be expressed in term of infinite series in (18) as follows

$$\mathscr{U}\left(x,t\right)=1+\cosh\left(2x\right)\left(\sum_{n=0}^{\infty}\frac{\left(-4it\right)^n}{n!}\right)=1+\cosh\left(2x\right)e^{-4it}, \tag{19}$$

which is in perfect accordance with the exact solution as in [60, 61, 65, 66].

Application 2. Consider the linear time-FSE [67]

$$\mathscr{D}_t^a\mathscr{U}+i\mathscr{U}_{xx}=0, \tag{20}$$

$subject to IC \mathscr{U}\left(x,0\right)=e^{3ix}$, where $a\in\left(0,1\right]$, $i^2=-1$, and the complex function $\mathscr{U}\left(x,t\right):\Omega\to\mathbb{C}$. The exact solutions when $a=1$ is $\mathscr{U}\left(x,t\right)=e^{3i(x+3t)}$. Following the analysis presented above, we can obtain the Laplace fractional equation for (20) as

$$\mathfrak{U}\left(x,\mathfrak{s}\right)=\frac{e^{3ix}}{\mathfrak{s}}-\frac{i}{\mathfrak{s}^a}\mathscr{L}\left\{\frac{\partial^2}{\partial x^2}\mathscr{L}^{-1}\left\{\mathfrak{U}\right\}\right\}. \tag{21}$$

Also, the $k-th$-truncated LFE series solution $\mathfrak{U}_k\left(x,\mathfrak{s}\right)$ for (21) can be expressed as

$$\mathfrak{U}_k\left(x,\mathfrak{s}\right)=\frac{e^{3ix}}{\mathfrak{s}}+\sum_{n=1}^{k}\frac{h_n\left(x\right)}{\mathfrak{s}^{na+1}}. \tag{22}$$

Next, based on the method, the $k-th$-truncated LFRE function of (21) can be defined as

$$\mathscr{L}\left(Res_{\mathfrak{U}_k}\left(x,\mathfrak{s}\right)\right)=\sum_{n=1}^{k}\frac{h_n\left(x\right)}{\mathfrak{s}^{na+1}}+\frac{i}{\mathfrak{s}^a}\mathscr{L}\left\{\frac{\partial^2}{\partial x^2}\mathscr{L}^{-1}\left\{\mathfrak{U}_k\right\}\right\}. \tag{23}$$

To get the $1-st$ LFRE function we let $k=1$ in (23). Therefore, one can obtain

$$\mathscr{L}\left(Res_{\mathfrak{U}_1}\left(x,\mathfrak{s}\right)\right)=\frac{h_1\left(x\right)}{\mathfrak{s}^{a+1}}+\frac{i}{\mathfrak{s}^a}\mathscr{L}\left\{\frac{\partial^2}{\partial x^2}\mathscr{L}^{-1}\left\{\frac{e^{3ix}}{\mathfrak{s}}+\frac{h_1\left(x\right)}{\mathfrak{s}^{a+1}}\right\}\right\}=\frac{h_1\left(x\right)-9ie^{3ix}}{\mathfrak{s}^{a+1}}+\frac{ih_1{}''\left(x\right)}{\mathfrak{s}^{2a+1}}. \tag{24}$$

By performing the following process $\lim_{\mathfrak{s}\to\infty}\mathfrak{s}^{a+1}\,\mathscr{L}\left(Res_{\mathfrak{U}_1}(x,\mathfrak{s})\right)=0$, it gives us $h_1(x)=9ie^{3ix}$. And so, the $1-st$ LFE series solution of (21) can be expressed as

$$\mathfrak{U}_1(x,\mathfrak{s})=\frac{e^{3ix}}{\mathfrak{s}}+\frac{9ie^{3ix}}{\mathfrak{s}^{a+1}}. \tag{25}$$

To get the $2-nd$ LFER function we let $k=2$ in (23), one can obtain

$$\mathscr{L}\left(Res_{\mathfrak{U}_2}(x,\mathfrak{s})\right)=\frac{9ie^{3ix}}{\mathfrak{s}^{a+1}}+\frac{h_2(x)}{\mathfrak{s}^{2a+1}}+\frac{i}{\mathfrak{s}^a}\mathscr{L}\left\{\frac{\partial^2}{\partial x^2}\mathscr{L}^{-1}\left\{\frac{e^{3ix}}{\mathfrak{s}}+\frac{9ie^{3ix}}{\mathfrak{s}^{a+1}}+\frac{h_2(x)}{\mathfrak{s}^{2a+1}}\right\}\right\}=\frac{h_2(x)-(9i)^2e^{3ix}}{\mathfrak{s}^{2a+1}}+\frac{ih_2{}''(x)}{\mathfrak{s}^{3a+1}}. \tag{26}$$

Performing the process $\lim_{\mathfrak{s}\to\infty}\mathfrak{s}^{2a+1}\,\mathscr{L}\left(Res_{\mathfrak{U}_2}(x,\mathfrak{s})\right)=0$ gives us that $h_2(x)=(9i)^2e^{3ix}$. Therefore, the 2-nd LFE series solution of (21) can be expressed as

$$\mathfrak{U}_3(x,\mathfrak{s})=\frac{e^{3ix}}{\mathfrak{s}}+\frac{9ie^{3ix}}{\mathfrak{s}^{a+1}}+\frac{(9i)^2e^{3ix}}{\mathfrak{s}^{2a+1}}. \tag{27}$$

The same matter for $k=3$ implies

$$\mathscr{L}\left(Res_{\mathfrak{U}_3}(x,\mathfrak{s})\right)=\frac{h_3(x)-(9i)^3e^{3ix}}{\mathfrak{s}^{3a+1}}+\frac{ih_3{}''(x)}{\mathfrak{s}^{4a+1}}. \tag{28}$$

Looking for the solution of $\lim_{\mathfrak{s}\to\infty}\mathfrak{s}^{3a+1}\,\mathscr{L}\left(Res_3(x,\mathfrak{s})\right)=0$ yields that $h_3(x)=(9i)^3e^{3ix}$. Hence, the $3-rd$ LFE series solution of (21) is

$$\mathfrak{U}_3(x,\mathfrak{s})=\frac{e^{3ix}}{\mathfrak{s}}+\frac{9ie^{3ix}}{\mathfrak{s}^{a+1}}+\frac{(9i)^2e^{3ix}}{\mathfrak{s}^{2a+1}}+\frac{(9i)^3e^{3ix}}{\mathfrak{s}^{3a+1}}. \tag{29}$$

In a similar way, the above process can be repeated smoothly using Mathematica for $k=4,5,6,\ldots$, and the fact $\lim_{\mathfrak{s}\to\infty}\mathfrak{s}^{ka+1}\,\mathscr{L}\left(Res_{\mathfrak{U}_k}(x,\mathfrak{s})\right)=0$ yields $h_k(x)=(9i)^ke^{3ix}$.

Consequently, if we collect the previous results, the $k-th$ truncated LFE series solution of (21) can be written in the following fractional expansion

$$\mathfrak{U}_k(x,\mathfrak{s})=\frac{e^{3ix}}{\mathfrak{s}}+\frac{9ie^{3ix}}{\mathfrak{s}^{a+1}}+\frac{(9i)^2e^{3ix}}{\mathfrak{s}^{2a+1}}+\frac{(9i)^3e^{3ix}}{\mathfrak{s}^{3a+1}}+\cdots+\frac{(9i)^ke^{3ix}}{\mathfrak{s}^{ka+1}}=e^{3ix}\left(\sum_{n=0}^{k}\frac{(9i)^n}{\mathfrak{s}^{na+1}}\right). \tag{30}$$

If we transform back expansion (30), one can get the $k-th$ truncated approximate solution of (20) as

$$\mathscr{U}_k(x,t)=e^{3ix}\left(\sum_{n=0}^{k}(9i)^n\frac{t^{na}}{\Gamma(na+1)}\right). \tag{31}$$

For the stander case $a=1$, the solution of (20) can be formulated in term of infinite series in (31) as follows

$$\mathscr{U}(x,t)=e^{3ix}\left(\sum_{n=0}^{\infty}\frac{(9it)^n}{n!}\right)=e^{3i(x+3t)}, \tag{32}$$

which is in perfect in accordance to the exact solution [67].

Application 3. Consider the nonlinear time-FSE [60, 65-67]

$$i\mathscr{D}_t^a\mathscr{U}+\mathscr{U}_{xx}+\psi|\mathscr{U}|^2\mathscr{U}=0, \tag{33}$$

subject to IC , $\mathscr{U}(x,0)=e^{\phi ix}$, where ψ, ϕ are two constant, $a\in(0,1]$, $i^2=-1$, $|\mathscr{U}|^2=\mathscr{U}\overline{\mathscr{U}}$, $\overline{\mathscr{U}}$, is the conjugate of $\mathscr{U}$, and the complex function $\mathscr{U}(x,t):\Omega\to\mathbb{C}$. The exact solutions for $a=1$ is $\mathscr{U}(x,t)=e^{i\left(\phi x+\left(\psi-\phi^2\right)t\right)}$.

Following the analysis presented above and multiply (33) by $-i$, we can obtain the Laplace fractional equation for (33) as

$$\mathfrak{U}(x,\mathfrak{s})=\frac{e^{\phi ix}}{\mathfrak{s}}+\frac{i}{\mathfrak{s}^a}\mathscr{L}\left\{\frac{\partial^2}{\partial x^2}\mathscr{L}^{-1}\{\mathfrak{U}\}\right\}+\frac{\psi i}{\mathfrak{s}^a}\mathscr{L}\left\{\left|\mathscr{L}^{-1}\{\mathfrak{U}\}\right|^2\mathscr{L}^{-1}\{\mathfrak{U}\}\right\}. \tag{34}$$

Further, the $k-th$-truncated LFE series solution $\mathfrak{U}_k(x,\mathfrak{s})$ for (34) can be expressed as

$$\mathfrak{U}_k(x,\mathfrak{s}) = \frac{e^{\phi ix}}{\mathfrak{s}} + \sum_{n=1}^{k} \frac{h_n(x)}{\mathfrak{s}^{na+1}}. \tag{35}$$

Next, based on the method, the $k-th$-truncated LFER of (34) can be written in the form

$$\mathscr{L}\left(Res_{\mathfrak{U}_k}(x,\mathfrak{s})\right) = \sum_{n=1}^{k} \frac{h_n(x)}{\mathfrak{s}^{na+1}} - \frac{i}{\mathfrak{s}^a}\mathscr{L}\left\{\frac{\partial^2}{\partial x^2}\mathscr{L}^{-1}\{\mathfrak{U}_k\}\right\} - \frac{\psi i}{\mathfrak{s}^a}\mathscr{L}\left\{\left|\mathscr{L}^{-1}\{\mathfrak{U}_k\}\right|^2\mathscr{L}^{-1}\{\mathfrak{U}_k\}\right\}. \tag{36}$$

To get the $1-st$ LFRE function we let $k=1$ in (36), one can obtain that

$$\mathscr{L}\left(Res_{\mathfrak{U}_1}(x,\mathfrak{s})\right) = \frac{h_1(x) - \left(\psi-\phi^2\right)ie^{\phi ix}}{\mathfrak{s}^{a+1}} + \frac{ih_1{}''(x) - 2\psi h_1(x) - \psi e^{2\phi ix}}{\mathfrak{s}^{2a+1}} - \psi\frac{2e^{\phi ix} - e^{-\phi ix}}{\mathfrak{s}^{3a+1}}\frac{\Gamma(1+2a)}{(\Gamma(1+a))^2}$$

$$-\psi\frac{h_1{}^2(x) - h_1{}^3(x)}{\mathfrak{s}^{4a+1}}\frac{\Gamma(1+3a)}{(\Gamma(1+a))^3}. \tag{37}$$

By performing the following process, $\lim_{\mathfrak{s}\to\infty}\mathfrak{s}^{a+1}\,\mathscr{L}\left(Res_{\mathfrak{U}_1}(x,\mathfrak{s})\right)=0$, which gives that $h_1(x)=\left(\psi-\phi^2\right)ie^{\phi ix}$. Hence, the $1-st$ LFE series solution of (34) can be expressed as

$$\mathfrak{U}_1(x,\mathfrak{s}) = \frac{e^{\phi ix}}{\mathfrak{s}} + \frac{\left(\psi-\phi^2\right)ie^{\phi ix}}{\mathfrak{s}^{a+1}}. \tag{38}$$

Remark 4.1. To find the $h_k(x)$ we multiply the $k-th$ LFRE function by $\mathfrak{s}^{ka+1}$. If $\theta > ka+1$, then by performing the process $\lim_{\mathfrak{s}\to\infty}\mathfrak{s}^{ka+1}\,\mathscr{L}\left(Res_{\mathfrak{U}_k}(x,\mathfrak{s})\right)=0$, any term divided by $\mathfrak{s}^{\omega}$, $\omega\geq\theta$ will be zero.
To get the 2nd LFRE we let $k=2$ in (36), one can obtain that:

$$\mathscr{L}\left(Res_{\mathfrak{U}_2}(x,\mathfrak{s})\right) = \frac{\left(\psi-\phi^2\right)ie^{nix}}{\mathfrak{s}^{a+1}} + \frac{h_2(x)}{\mathfrak{s}^{2a+1}} - \frac{i}{\mathfrak{s}^a}\mathscr{L}\left\{\frac{\partial^2}{\partial x^2}\mathscr{L}^{-1}\left\{\frac{e^{\phi ix}}{\mathfrak{s}} + \frac{\left(\psi-\phi^2\right)ie^{\phi ix}}{\mathfrak{s}^{a+1}} + \frac{h_2(x)}{\mathfrak{s}^{2a+1}}\right\}\right\} - \frac{\psi i}{\mathfrak{s}^a}\mathscr{L}.$$

$$-\frac{\psi i}{\mathfrak{s}^a}\mathscr{L}\left\{\left|\mathscr{L}^{-1}\left\{\frac{e^{\phi ix}}{\mathfrak{s}} + \frac{\left(\psi-\phi^2\right)ie^{\phi ix}}{\mathfrak{s}^{a+1}} + \frac{h_2(x)}{\mathfrak{s}^{2a+1}}\right\}\right|^2\mathscr{L}^{-1}\left\{\frac{e^{\phi ix}}{\mathfrak{s}} + \frac{\left(\psi-\phi^2\right)ie^{nix}}{\mathfrak{s}^{a+1}} + \frac{h_2(x)}{\mathfrak{s}^{2a+1}}\right\}\right\} \tag{39}$$

By performing the process $\lim_{\mathfrak{s}\to\infty}\mathfrak{s}^{2a+1}\,\mathscr{L}\left(Res_{\mathfrak{U}_2}(x,\mathfrak{s})\right)=0$, and by using Remark 1, $h_2(x)=\left(\left(\psi-\phi^2\right)i\right)^2e^{\phi ix}$. Thus, the 2-nd

LFE series solution of (34) can be expressed as

$$\mathfrak{U}_3(x,\mathfrak{s}) = \frac{e^{\phi ix}}{\mathfrak{s}} + \frac{\left(\psi-\phi^2\right)ie^{nix}}{\mathfrak{s}^{a+1}} + \frac{\left(\left(\psi-\phi^2\right)i\right)^2e^{\phi ix}}{\mathfrak{s}^{2a+1}}. \tag{40}$$

The same matter for $k=3$ reveals

$$\mathscr{L}\left(Res_{\mathfrak{U}_3}(x,\mathfrak{s})\right) = \frac{\left(\psi-\phi^2\right)ie^{nix}}{\mathfrak{s}^{a+1}} + \frac{\left(\left(\psi-\phi^2\right)i\right)^2e^{\phi ix}}{\mathfrak{s}^{2a+1}} + \frac{h_3(x)}{\mathfrak{s}^{3a+1}}$$

$$-\frac{i}{\mathfrak{s}^a}\mathscr{L}\left\{\frac{\partial^2}{\partial x^2}\mathscr{L}^{-1}\left\{\frac{e^{\phi ix}}{\mathfrak{s}} + \frac{\left(\psi-\phi^2\right)ie^{\phi ix}}{\mathfrak{s}^{a+1}} + \frac{\left(\left(\psi-\phi^2\right)i\right)^2e^{\phi ix}}{\mathfrak{s}^{2a+1}} + \frac{h_3(x)}{\mathfrak{s}^{3a+1}}\right\}\right\} - \frac{\psi i}{\mathfrak{s}^a}\mathscr{L}$$

$$\left\{\left|\mathscr{L}^{-1}\left\{\frac{e^{\phi ix}}{\mathfrak{s}} + \frac{\left(\left(\psi-\phi^2\right)i\right)^2e^{\phi ix}}{\mathfrak{s}^{2a+1}} + \frac{h_3(x)}{\mathfrak{s}^{3a+1}}\right\}\right|^2\mathscr{L}^{-1}\left\{\frac{e^{\phi ix}}{\mathfrak{s}} + ... + \frac{\left(\left(\psi-\phi^2\right)i\right)^2e^{\phi ix}}{\mathfrak{s}^{2a+1}} + \frac{h_3(x)}{\mathfrak{s}^{3a+1}}\frac{\left(\psi-\phi^2\right)ie^{\phi ix}}{\mathfrak{s}^{a+1}} + \frac{h_2(x)}{\mathfrak{s}^{2a+1}}\right\}\right\} \tag{41}$$

Looking for the solution of $\lim_{\mathfrak{s}\to\infty}\mathfrak{s}^{3a+1}\,\mathscr{L}\left(Res_3\left(x,\mathfrak{s}\right)\right)=0$ give us that $h_3\left(x\right)=\left(\left(\psi-\phi^2\right)i\right)^3e^{\phi ix}$. Hence, by Remark 4.1, the $3-rd$ LFE series solution of (34) becomes

$$\mathfrak{U}_3\left(x,\mathfrak{s}\right)=\frac{e^{\phi ix}}{\mathfrak{s}}+\frac{\left(\psi-\phi^2\right)ie^{\phi ix}}{\mathfrak{s}^{a+1}}+\frac{\left(\left(\psi-\phi^2\right)i\right)^2e^{\phi ix}}{\mathfrak{s}^{2a+1}}+\frac{\left(\left(\psi-\phi^2\right)i\right)^3e^{\phi ix}}{\mathfrak{s}^{3a+1}},\tag{42}$$

Similarly, the above process can be repeated smoothly using Mathematica for $k=4,5,6,\ldots$, and since $\lim_{\mathfrak{s}\to\infty}\mathfrak{s}^{ka+1}\,\mathscr{L}\left(Res_{\mathfrak{U}_k}\left(x,\mathfrak{s}\right)\right)=0$, we have $h_k\left(x\right)=\left(\left(\psi-\phi^2\right)i\right)^ke^{\phi ix}$.
Consequently, if we collect all the previous results, the $k-th$ LFE series solution of (34) can be written as

$$\begin{aligned}\mathfrak{U}_k\left(x,\mathfrak{s}\right)&=\frac{e^{\phi ix}}{\mathfrak{s}}+\frac{\left(\psi-\phi^2\right)ie^{nix}}{\mathfrak{s}^{a+1}}+\frac{\left(\left(\psi-\phi^2\right)i\right)^2e^{\phi ix}}{\mathfrak{s}^{2a+1}}+\frac{\left(\left(\psi-\phi^2\right)i\right)^3e^{\phi ix}}{\mathfrak{s}^{3a+1}}+\cdots+\frac{\left(\left(\psi-\phi^2\right)i\right)^ke^{\phi ix}}{\mathfrak{s}^{ka+1}}\\&=e^{\phi ix}\left(\sum_{n=0}^{k}\frac{\left(\left(\psi-\phi^2\right)i\right)^n}{\mathfrak{s}^{na+1}}\right).\end{aligned}\tag{43}$$

If we transform back expansion (34), one can get the $k-th$ truncated approximate solution of (33) in the form

$$\mathscr{U}_k\left(x,t\right)=e^{\phi ix}\left(\sum_{n=0}^{k}\left(\left(\psi-\phi^2\right)i\right)^n\frac{t^{na}}{\Gamma\left(na+1\right)}\right).\tag{44}$$

For the stander case $a=1$ and in term of infinite series in (44), the solution of (33) can be written as

$$\mathscr{U}\left(x,t\right)=e^{\phi ix}\left(\sum_{n=0}^{\infty}\frac{\left(\left(\psi-\phi^2\right)it\right)^n}{n!}\right)=e^{\phi ix}e^{\left(\left(\psi-\phi^2\right)it\right)}=e^{i\left(\phi x+\left(\psi-\phi^2\right)t\right)},\tag{45}$$

which is in perfect accordance with the exact solution [60, 65-67].
Application 4. Consider the cubic nonlinear time-FSE [60, 62-65, 67]:

$$i\mathscr{D}_t^a\mathscr{U}+\frac{1}{2}\mathscr{U}_{xx}-\mathscr{U}\cos^2x-\left|\mathscr{U}\right|^2\mathscr{U}=0,\tag{46}$$

subject to IC: $\mathscr{U}\left(x,0\right)=\sin x$, where $\in(0,1]$, $i^2=-1$, $\left|\mathscr{U}\right|^2=\mathscr{U}\overline{\mathscr{U}}$, $\overline{\mathscr{U}}$ is the conjugate of $\mathscr{U}$, and the complex function $\mathscr{U}\left(x,t\right):\Omega\to\mathbb{C}$. The exact solutions when $a=1$ is $\mathscr{U}\left(x,t\right)=\sin x\,e^{\frac{-3i}{2}t}$.

Following the analysis presented above, and upon multiplying (46) by $-i$, we can obtain the Laplace fractional equation for (46) as

$$\mathfrak{U}\left(x,\mathfrak{s}\right)=\frac{\sin x}{\mathfrak{s}}+\frac{i}{2\mathfrak{s}^a}\mathscr{L}\left\{\frac{\partial^2}{\partial x^2}\mathscr{L}^{-1}\left\{\mathfrak{U}\right\}\right\}-\frac{i}{\mathfrak{s}^a}\mathscr{L}\left\{\mathscr{L}^{-1}\left\{\mathfrak{U}\right\}\right\}\cos^2x-\frac{i}{\mathfrak{s}^a}\mathscr{L}\left\{\left|\mathscr{L}^{-1}\left\{\mathfrak{U}\right\}\right|^2\right\}\mathscr{L}\left\{\mathscr{L}^{-1}\left\{\mathfrak{U}\right\}\right\}.\tag{47}$$

Moreover, the $k-th$ LFE series solution $\mathfrak{U}_k\left(x,\mathfrak{s}\right)$ for (47) can be written as

$$\mathfrak{U}_k\left(x,\mathfrak{s}\right)=\frac{\sin x}{\mathfrak{s}}+\sum_{n=1}^{k}\frac{h_n\left(x\right)}{\mathfrak{s}^{na+1}}.\tag{48}$$

Next, based on the method, the $k-th$ LFRE function of (47) can be defined in the form

$$\mathscr{L}\left(Res_{\mathfrak{U}_k}\left(x,\mathfrak{s}\right)\right)=\sum_{n=1}^{k}\frac{h_n\left(x\right)}{\mathfrak{s}^{na+1}}-\frac{i}{2\mathfrak{s}^a}\mathscr{L}\left\{\frac{\partial^2}{\partial x^2}\mathscr{L}^{-1}\left\{\mathfrak{U}_k\right\}\right\}+\frac{i}{\mathfrak{s}^a}\mathscr{L}\left\{\mathscr{L}^{-1}\left\{\mathfrak{U}_k\right\}\right\}\cos^2x+\frac{i}{\mathfrak{s}^a}\mathscr{L}\left\{\left|\mathscr{L}^{-1}\left\{\mathfrak{U}_k\right\}\right|^2\right\}\mathscr{L}\left\{\mathscr{L}^{-1}\left\{\mathfrak{U}_k\right\}\right\}.\tag{49}$$

To get the $1-st$ LRFE function we put $k=1$ in (49) to have

$$\lim_{\mathfrak{s}\to\infty}\mathfrak{s}^{a+1}\,\mathscr{L}\left(Res_{\mathfrak{U}_1}\left(x,\mathfrak{s}\right)\right)=h_1\left(x\right)+\frac{3i}{2}\sin x\,.\tag{50}$$

By performing the following process $\lim_{\mathfrak{s}\to\infty}\mathfrak{s}^{a+1}\,\mathscr{L}\left(Res_{\mathfrak{U}_1}\left(x,\mathfrak{s}\right)\right)=0$, we establish that $h_1\left(x\right)=-\frac{3i}{2}\sin x$. Hence, the $1-st$ LFE series solution of (47) can be expressed as

$$\mathfrak{U}_1\left(x,\mathfrak{s}\right)=\frac{\sin x}{\mathfrak{s}}+\left(-\frac{3i}{2}\right)\frac{\sin x}{\mathfrak{s}^{a+1}}.\tag{51}$$

To get the $2-nd$ LFRE function we let $k=2$ in (49), one can obtain that:

$$\lim_{\mathfrak{s}\to\infty}\mathfrak{s}^{2a+1}\,\mathscr{L}\left(Res_{\mathfrak{U}_2}(x,\mathfrak{s})\right)=h_2(x)+\frac{9}{4}\sin x\,. \tag{52}$$

By performing the following process, $\lim_{\mathfrak{s}\to\infty}\mathfrak{s}^{2a+1}\,\mathscr{L}\left(Res_{\mathfrak{U}_2}(x,\mathfrak{s})\right)=0$, and by Remark 4.1, $h_2(x)=-\frac{9}{4}\sin x$. So, the $2-nd$ LFE series solution of (**??**) can be expressed as

$$\mathfrak{U}_2(x,\mathfrak{s})=\frac{\sin x}{\mathfrak{s}}+\left(-\frac{3i}{2}\right)\frac{\sin x}{\mathfrak{s}^{a+1}}+\left(-\frac{3i}{2}\right)^2\frac{\sin x}{\mathfrak{s}^{2a+1}}. \tag{53}$$

The same matter for $k=3$ implies

$$\lim_{\mathfrak{s}\to\infty}\mathfrak{s}^{3a+1}\,\mathscr{L}\left(Res_{\mathfrak{U}_3}(x,\mathfrak{s})\right)=h_3(x)-\frac{27i}{8}\sin x\,. \tag{54}$$

By solving $\lim_{\mathfrak{s}\to\infty}\mathfrak{s}^{3a+1}\,\mathscr{L}\left(Res_3(x,\mathfrak{s})\right)=0$, we obtain that $h_3(x)=\left(-\frac{3i}{2}\right)^3\sin x$. Hence, by Remark 4.1, the $3-rd$ Laplace series solution of (47) becomes

$$\mathfrak{U}_3(x,\mathfrak{s})=\frac{\sin x}{\mathfrak{s}}+\left(-\frac{3i}{2}\right)\frac{\sin x}{\mathfrak{s}^{a+1}}+\left(-\frac{3i}{2}\right)^2\frac{\sin x}{\mathfrak{s}^{2a+1}}+\left(-\frac{3i}{2}\right)^3\frac{\sin x}{\mathfrak{s}^{3a+1}}. \tag{55}$$

In a similar manner, the above process can be repeated smoothly using Mathematica for $k=4,5,6,\ldots$, and the fact that $\lim_{\mathfrak{s}\to\infty}\mathfrak{s}^{ka+1}\,\mathscr{L}\left(Res_{\mathfrak{U}_k}(x,\mathfrak{s})\right)=0$ leads to $h_k(x)=\left(-\frac{3i}{2}\right)^k\sin x$.
Consequently, if we collect all the previous results, the $k-th$ LFE series solution of (47) can be written as

$$\mathfrak{U}_k(x,\mathfrak{s})=\frac{\sin x}{\mathfrak{s}}+\left(-\frac{3i}{2}\right)\frac{\sin x}{\mathfrak{s}^{a+1}}+\left(-\frac{3i}{2}\right)^2\frac{\sin x}{\mathfrak{s}^{2a+1}}+\left(-\frac{3i}{2}\right)^3\frac{\sin x}{\mathfrak{s}^{3a+1}}+\cdots+\left(-\frac{3i}{2}\right)^k\frac{\sin x}{\mathfrak{s}^{ka+1}}=\sin x\left(\sum_{n=0}^{k}\frac{\left(-\frac{3i}{2}\right)^n}{\mathfrak{s}^{na+1}}\right). \tag{56}$$

If we transform back the expansion (56), one can get that the $k-th$ truncated approximate solution of (46) has the following expansion

$$\mathscr{U}_k(x,t)=\sin x\left(\sum_{n=0}^{k}\left(-\frac{3i}{2}\right)^n\frac{t^{na}}{\Gamma(na+1)}\right). \tag{57}$$

For the case $a=1$ and in term of infinite series in (57), the solution of (**??**) can be expressed as follows

$$\mathscr{U}(x,t)=\sin x\left(\sum_{n=0}^{\infty}\frac{\left(-\frac{3i}{2}t\right)^n}{n!}\right)=\sin x\,e^{-\frac{3i}{2}t}, \tag{58}$$

which is in perfect accordance with the exact solution as in [60, 62-65, 67].

5 Numerical and Graphical Results

This section is devoted to study numerical and graphical simulations of the examined Caputo time-FSEs via Laplace fractional RPS technique. The merit of utilizing the present algorithm is to attain exact and approximate solutions in a simple fashion with no assumptions on the constructed model. As well, it is provide a rapid convergence with minimal computational work compared to other techniques. 2D, and 3D graphs for different FD values are plotted for giving a clear conception of the dynamic behavior of considered models. To demonstrate the simplicity and efficiency of the recommended scheme, errors of the approximate solution and some numerical comparisons are conducted and summarized.

Following, are some graphically and numerically representatives for Applications 3, and 4. Tables 1 and 2 display the absolute error between the $5-th$ approximate and exact solutions of the real and imaginary parts of $\mathscr{U}(x,t)$ for Application 3, respectively, at $\psi=2$, $\phi=1$, $x=0.3$ and $x=0.2$, with a value of 1 for a and t ranging from 0 to 1. It is worth noting that the results were identical to those of other methods, as shown in Tables 1 and 2. Tables 3 and 4 compare the absolute error of the $5-th$ approximate solutions for the real and imaginary parts, respectively, with other methods for Application 3 at $=2$, $\phi=1$, $t=0.1$, x ranging from 0 to 1, and a values of 0.7, 0.8, and 0.9. The results obtained using

Laplace fractional RPS method are better than those obtained using other methods. Similarly, Tables 5 and 6 compare the absolute error of the $5-th$ approximate solutions for the real and imaginary parts, respectively, with other methods for Application 4 at $t=0.1$, x ranging from 0 to 1, and a values of 0.7, 0.8, and 0.9. The results obtained using Laplace fractional RPS method are better than those obtained using other methods.

Figs. 1 and 2 depict the impact of the variable x and the fractional-order derivative a on the solution profile by showing the exact and approximate solutions. The 2D graphs in Figs. 1 and 2 display the $5-th$ approximate solutions achieved by Laplace fractional RPS method with $t=0.3$ at fractional-order derivative values of $a=0.6$, 0.7, 0.8, 0.9, and 1, along with the exact solutions for Applications 3 when $\psi=2$, $\phi=1$ and 4, respectively. The figures demonstrate that the approximate solutions obtained by Laplace fractional RPS method are more accurate as a approaches 1, with the approximate solutions closely matching the exact solutions at $a=1$. This provides evidence of the effectiveness and precision of the proposed method.

Figs. 3-6 present 3D-graphs of the $5-th$ approximate solutions derived using Laplace fractional RPS method at different values of $a=0.6$, 0.7, 0.8, 0.9 for Applications 3, and 4 at $\psi=2$, $\phi=1$ and 4, along with their exact solutions. These figures demonstrate that the approximate solutions obtained using Laplace fractional RPS method become increasingly like the exact solutions as a approaches 1. Moreover, the approximate solutions coincide with the exact solutions at $a=1$, which confirms the effectiveness of the recommended method. Based on the graphical results, it can be concluded that the suggested approach produces highly accurate solutions in the form of a series with minimal computational effort.

Table 1. The absolute error comparison with various approaches for Application 3 when $=2$, $\phi=1$, $a=1$, $x=0.3$, and $n=5$

t_i	**Exact of the real part of** $\mathscr{U}(x,t)$	**Abs. error of the real part of** $\mathscr{U}_5(x,t)$	**Abs. error of the real part of** $\mathscr{U}_5(x,t)$	**Exact of the imaginary part of** $\mathscr{U}(x,t)$	**Abs. error of the imaginary part of** $\mathscr{U}_5(x,t)$	**Abs. error of the imaginary part of** $\mathscr{U}_5(x,t)$
		Present Method	**[60]**		**Present Method**	**[60]**
0.05	9.39373×10^{-1}	2.06853×10^{-11}	2.06853×10^{-11}	3.42898×10^{-1}	6.56092×10^{-12}	6.56092×10^{-12}
0.15	9.00447×10^{-1}	1.50075×10^{-8}	1.50075×10^{-8}	4.34966×10^{-1}	4.99711×10^{-9}	4.99711×10^{-9}
0.25	8.52525×10^{-1}	3.20003×10^{-7}	3.20003×10^{-7}	5.22687×10^{-1}	1.11654×10^{-7}	1.11654×10^{-7}
0.35	7.96084×10^{-1}	2.39612×10^{-6}	2.39612×10^{-6}	6.05186×10^{-1}	8.74607×10^{-7}	8.74607×10^{-7}
0.45	7.31689×10^{-1}	1.07597×10^{-5}	1.07597×10^{-5}	6.81639×10^{-1}	4.10225×10^{-6}	4.10225×10^{-6}
0.55	6.59983×10^{-1}	3.56416×10^{-5}	3.56416×10^{-5}	7.51280×10^{-1}	1.41739×10^{-5}	1.41739×10^{-5}
0.65	5.81683×10^{-1}	9.64609×10^{-5}	9.64609×10^{-5}	8.13416×10^{-1}	3.99607×10^{-5}	3.99607×10^{-5}
0.75	4.97571×10^{-1}	2.60290×10^{-4}	2.60290×10^{-4}	8.67423×10^{-1}	9.74265×10^{-5}	9.74265×10^{-5}
0.85	4.08487×10^{-1}	4.75409×10^{-4}	4.75409×10^{-4}	9.12764×10^{-1}	2.12978×10^{-4}	2.12978×10^{-4}
0.95	3.15322×10^{-1}	9.19361×10^{-4}	9.19361×10^{-4}	9.48985×10^{-1}	4.27625×10^{-4}	4.27625×10^{-4}

Table 2. The absolute error comparison with various approaches for Application 3 when $= 2,\ \phi = 1$, $a = 1$, $x = 0.2$, and $n = 5$.

t_i	**Exact of the real part of** $\mathscr{U}(x,t)$	**Abs. error of the real part of** $\mathscr{U}_5(x,t)$	**Abs. error of the real part of** $\mathscr{U}_5(x,t)$	**Exact of the imaginary part of** $\mathscr{U}(x,t)$	**Abs. error of the imaginary part of** $\mathscr{U}_5(x,t)$	**Abs. error of the imaginary part of** $\mathscr{U}_5(x,t)$
		Present Method	**[60]**		**Present Method**	**[60]**
0.1	$\mathbf{9.55336 \times 10^{-1}}$	$1.35702 \times \mathbf{10^{-9}}$	$1.35702 \times \mathbf{10^{-9}}$	$\mathbf{2.95520 \times 10^{-1}}$	$2.95323 \times \mathbf{10^{-10}}$	$2.95323 \times \mathbf{10^{-10}}$
0.2	$\mathbf{9.21061 \times 10^{-1}}$	$8.65506 \times \mathbf{10^{-8}}$	$8.65506 \times \mathbf{10^{-8}}$	$\mathbf{3.89418 \times 10^{-1}}$	$2.01346 \times \mathbf{10^{-8}}$	$2.01346 \times \mathbf{10^{-8}}$
0.3	$\mathbf{8.77583 \times 10^{-1}}$	$9.82114 \times \mathbf{10^{-7}}$	$9.82114 \times \mathbf{10^{-7}}$	$\mathbf{4.79426 \times 10^{-1}}$	$2.43305 \times \mathbf{10^{-7}}$	$2.43305 \times \mathbf{10^{-7}}$
0.4	$\mathbf{8.25336 \times 10^{-1}}$	$5.49515 \times \mathbf{10^{-6}}$	$5.49515 \times \mathbf{10^{-6}}$	$\mathbf{5.64642 \times 10^{-1}}$	$1.44488 \times \mathbf{10^{-6}}$	$1.44488 \times \mathbf{10^{-6}}$
0.5	$\mathbf{7.64842 \times 10^{-1}}$	$2.08672 \times \mathbf{10^{-5}}$	$2.08672 \times \mathbf{10^{-5}}$	$\mathbf{6.44218 \times 10^{-1}}$	$5.80614 \times \mathbf{10^{-6}}$	$5.80614 \times \mathbf{10^{-6}}$
0.6	$\mathbf{6.96707 \times 10^{-1}}$	$6.20037 \times \mathbf{10^{-5}}$	$6.20037 \times \mathbf{10^{-5}}$	$\mathbf{7.17356 \times 10^{-1}}$	$1.82078 \times \mathbf{10^{-5}}$	$1.82078 \times \mathbf{10^{-5}}$
0.7	$\mathbf{6.21610 \times 10^{-1}}$	$1.55526 \times \mathbf{10^{-4}}$	$1.55526 \times \mathbf{10^{-4}}$	$\mathbf{7.83327 \times 10^{-1}}$	$4.80863 \times \mathbf{10^{-5}}$	$4.80863 \times \mathbf{10^{-5}}$
0.8	$\mathbf{5.40302 \times 10^{-1}}$	$3.44589 \times \mathbf{10^{-4}}$	$3.44589 \times \mathbf{10^{-4}}$	$\mathbf{8.41471 \times 10^{-1}}$	$1.11933 \times \mathbf{10^{-4}}$	$1.11933 \times \mathbf{10^{-4}}$
0.9	$\mathbf{4.53596 \times 10^{-1}}$	$6.94386 \times \mathbf{10^{-4}}$	$6.94386 \times \mathbf{10^{-4}}$	$\mathbf{8.91207 \times 10^{-1}}$	$2.36508 \times \mathbf{10^{-4}}$	$2.36508 \times \mathbf{10^{-4}}$
1.0	$\mathbf{3.62358 \times 10^{-1}}$	$1.29829 \times \mathbf{10^{-3}}$	$1.29829 \times \mathbf{10^{-3}}$	$\mathbf{9.32039 \times 10^{-1}}$	$4.62838 \times \mathbf{10^{-4}}$	$4.62838 \times \mathbf{10^{-4}}$

Table 3. The absolute error comparison with other method for the real part at various values of a for Application 3 when $= 2,\ \phi = 1$, $t = 0.1$, and $n = 5$.

x_i	$\mathscr{U}_5(x,t)$	$\mathscr{U}_5(x,t)$	$\mathscr{U}_5(x,t)$	$\mathscr{U}_5(x,t)$	$\mathscr{U}_5(x,t)$	$\mathscr{U}_5(x,t)$
	a=0.7	a=0.7	a=0.8	a=0.8	a=0.9	a=0.9
	Present Method	**[60]**	**Present Method**	**[60]**	**Present Method**	**[60]**
0.1	$\mathbf{3.81798 \times 10^{-2}}$	$5.32815 \times \mathbf{10^{-2}}$	$\mathbf{1.93192 \times 10^{-2}}$	$2.41737 \times \mathbf{10^{-2}}$	$\mathbf{7.47036 \times 10^{-3}}$	$8.70022 \times \mathbf{10^{-3}}$
0.2	$\mathbf{4.92622 \times 10^{-2}}$	$7.06783 \times \mathbf{10^{-2}}$	$\mathbf{2.59524 \times 10^{-2}}$	$3.35417 \times \mathbf{10^{-2}}$	$\mathbf{1.04271 \times 10^{-2}}$	$1.25420 \times \mathbf{10^{-2}}$
0.3	$\mathbf{5.98525 \times 10^{-2}}$	$8.73689 \times \mathbf{10^{-2}}$	$\mathbf{3.23262 \times 10^{-2}}$	$4.25746 \times \mathbf{10^{-2}}$	$\mathbf{1.32796 \times 10^{-2}}$	$1.62585 \times \mathbf{10^{-2}}$
0.4	$\mathbf{6.98447 \times 10^{-2}}$	$1.03187 \times \mathbf{10^{-1}}$	$\mathbf{3.83771 \times 10^{-2}}$	$5.11821 \times \mathbf{10^{-2}}$	$\mathbf{1.59994 \times 10^{-2}}$	$1.98125 \times \mathbf{10^{-2}}$
0.5	$\mathbf{7.91390 \times 10^{-2}}$	$1.17973 \times \mathbf{10^{-1}}$	$\mathbf{4.40444 \times 10^{-2}}$	$5.92782 \times \mathbf{10^{-2}}$	$\mathbf{1.85594 \times 10^{-2}}$	$2.31685 \times \mathbf{10^{-2}}$
0.6	$\mathbf{8.76426 \times 10^{-2}}$	$1.31581 \times \mathbf{10^{-1}}$	$\mathbf{4.92718 \times 10^{-2}}$	$6.67820 \times \mathbf{10^{-2}}$	$\mathbf{2.09339 \times 10^{-2}}$	$2.62931 \times \mathbf{10^{-2}}$
0.7	$\mathbf{9.52705 \times 10^{-2}}$	$1.43874 \times \mathbf{10^{-1}}$	$\mathbf{5.40068 \times 10^{-2}}$	$7.36186 \times \mathbf{10^{-2}}$	$\mathbf{2.30992 \times 10^{-2}}$	$2.91550 \times \mathbf{10^{-2}}$
0.8	$\mathbf{1.01946 \times 10^{-1}}$	$1.54730 \times \mathbf{10^{-1}}$	$\mathbf{5.82021 \times 10^{-2}}$	$7.97196 \times \mathbf{10^{-2}}$	$\mathbf{2.50338 \times 10^{-2}}$	$3.17255 \times \mathbf{10^{-2}}$
0.9	$\mathbf{1.07604 \times 10^{-1}}$	$1.64040 \times \mathbf{10^{-1}}$	$\mathbf{6.18160 \times 10^{-2}}$	$8.50240 \times \mathbf{10^{-2}}$	$\mathbf{2.67182 \times 10^{-2}}$	$3.17255 \times \mathbf{10^{-2}}$
1.0	$\mathbf{1.12186 \times 10^{-1}}$	$1.71710 \times \mathbf{10^{-1}}$	$\mathbf{6.48122 \times 10^{-2}}$	$8.94790 \times \mathbf{10^{-2}}$	$\mathbf{2.81357 \times 10^{-2}}$	$3.58931 \times \mathbf{10^{-2}}$

Table 4. The absolute error comparison with other method for the imaginary part at various values of a for Application 3 when $= 2$, $\phi = 1$, $t = 0.1$, and $n = 5$.

x_i	$\mathscr{U}_5(x,t)$	$\mathscr{U}_5(x,t)$	$\mathscr{U}_5(x,t)$	$\mathscr{U}_5(x,t)$	$\mathscr{U}_5(x,t)$	$\mathscr{U}_5(x,t)$
	a=0.7	a=0.7	a=0.8	a=0.8	a=0.9	a=0.9
	Present Method	**[60]**	**Present Method**	**[60]**	**Present Method**	**[60]**
0.1	**1.12920** $\times$ **10^{-1}**	1.76925 $\times$ **10^{-1}**	**6.74088** $\times$ **10^{-2}**	9.50464 $\times$ **10^{-2}**	**2.99901** $\times$ **10^{-2}**	3.89173 $\times$ **10^{-2}**
0.2	**1.08544** $\times$ **10^{-1}**	1.70721 $\times$ **10^{-1}**	**6.51434** $\times$ **10^{-2}**	9.21582 $\times$ **10^{-2}**	**2.90945** $\times$ **10^{-2}**	3.78543 $\times$ **10^{-2}**
0.3	**1.03084** $\times$ **10^{-1}**	1.62813 $\times$ **10^{-1}**	**6.22270** $\times$ **10^{-2}**	8.83492 $\times$ **10^{-2}**	**2.79082** $\times$ **10^{-2}**	3.64131 $\times$ **10^{-2}**
0.4	**9.65936** $\times$ **10^{-2}**	1.53277 $\times$ **10^{-1}**	**5.86889** $\times$ **10^{-2}**	8.36574 $\times$ **10^{-2}**	**2.64430** $\times$ **10^{-2}**	3.46080 $\times$ **10^{-2}**
0.5	**8.91382** $\times$ **10^{-2}**	1.42210 $\times$ **10^{-1}**	**5.45644** $\times$ **10^{-2}**	7.81298 $\times$ **10^{-2}**	**2.47136** $\times$ **10^{-2}**	3.24572 $\times$ **10^{-2}**
0.6	**8.07921** $\times$ **10^{-2}**	1.29721 $\times$ **10^{-1}**	**4.98947** $\times$ **10^{-2}**	7.18215 $\times$ **10^{-2}**	**2.27373** $\times$ **10^{-2}**	2.99821 $\times$ **10^{-2}**
0.7	**7.16388** $\times$ **10^{-2}**	1.15937 $\times$ **10^{-1}**	**4.47265** $\times$ **10^{-2}**	6.47957 $\times$ **10^{-2}**	**2.05338** $\times$ **10^{-2}**	2.72073 $\times$ **10^{-2}**
0.8	**6.17698** $\times$ **10^{-2}**	1.00995 $\times$ **10^{-1}**	**3.91113** $\times$ **10^{-2}**	5.71224 $\times$ **10^{-2}**	**1.81252** $\times$ **10^{-2}**	2.41608 $\times$ **10^{-2}**
0.9	**5.12835** $\times$ **10^{-2}**	8.50428 $\times$ **10^{-2}**	**3.31054** $\times$ **10^{-2}**	4.88783 $\times$ **10^{-2}**	**1.55354** $\times$ **10^{-2}**	2.08728 $\times$ **10^{-2}**
1.0	**4.02848** $\times$ **10^{-2}**	6.82413 $\times$ **10^{-2}**	**2.67687** $\times$ **10^{-2}**	4.01459 $\times$ **10^{-2}**	**1.27904** $\times$ **10^{-2}**	1.73763 $\times$ **10^{-2}**

Table 5. The absolute error comparison with other method for the real part at various values of a for Application 4 when $t = 0.1$, and $n = 5$.

x_i	$\mathscr{U}_5(x,t)$	$\mathscr{U}_5(x,t)$	$\mathscr{U}_5(x,t)$	$\mathscr{U}_5(x,t)$	$\mathscr{U}_5(x,t)$	$\mathscr{U}_5(x,t)$
	a=0.7	a=0.7	a=0.8	a=0.8	a=0.9	a=0.9
	Present Method	**[60]**	**Present Method**	**[60]**	**Present Method**	**[60]**
0.1	**5.90743** $\times$ **10^{-3}**	**7.86580** $\times$ **10^{-3}**	**2.78459** $\times$ **10^{-3}**	**3.25470** $\times$ **10^{-3}**	**9.93016** $\times$ **10^{-4}**	**1.06850** $\times$ **10^{-3}**
0.2	**1.17558** $\times$ **10^{-2}**	**1.56530** $\times$ **10^{-2}**	**5.54135** $\times$ **10^{-3}**	**6.47689** $\times$ **10^{-3}**	**1.97611** $\times$ **10^{-3}**	**2.12633** $\times$ **10^{-3}**
0.3	**1.74868** $\times$ **10^{-2}**	**2.32838** $\times$ **10^{-2}**	**8.24275** $\times$ **10^{-3}**	**9.63436** $\times$ **10^{-3}**	**2.93946** $\times$ **10^{-3}**	**3.16291** $\times$ **10^{-3}**
0.4	**2.30430** $\times$ **10^{-2}**	**3.06820** $\times$ **10^{-2}**	**1.08618** $\times$ **10^{-2}**	**1.26956** $\times$ **10^{-2}**	**3.87344** $\times$ **10^{-3}**	**1.67880** $\times$ **10^{-3}**
0.5	**2.83690** $\times$ **10^{-2}**	**3.77736** $\times$ **10^{-2}**	**1.33723** $\times$ **10^{-2}**	**1.56299** $\times$ **10^{-2}**	**4.76871** $\times$ **10^{-3}**	**5.13122** $\times$ **10^{-3}**
0.6	**3.34115** $\times$ **10^{-2}**	**4.44878** $\times$ **10^{-2}**	**1.57492** $\times$ **10^{-2}**	**1.84081** $\times$ **10^{-2}**	**5.61634** $\times$ **10^{-3}**	**6.04328** $\times$ **10^{-3}**
0.7	**3.81202** $\times$ **10^{-2}**	**5.07575** $\times$ **10^{-2}**	**1.79687** $\times$ **10^{-2}**	**2.10024** $\times$ **10^{-2}**	**6.40786** $\times$ **10^{-3}**	**6.89496** $\times$ **10^{-3}**
0.8	**4.24480** $\times$ **10^{-2}**	**5.65200** $\times$ **10^{-2}**	**2.00087** $\times$ **10^{-2}**	**2.33868** $\times$ **10^{-2}**	**7.13534** $\times$ **10^{-3}**	**7.67775** $\times$ **10^{-3}**
0.9	**4.63517** $\times$ **10^{-2}**	**6.17178** $\times$ **10^{-2}**	**2.18488** $\times$ **10^{-2}**	**2.55375** $\times$ **10^{-2}**	**7.79154** $\times$ **10^{-3}**	**8.38383** $\times$ **10^{-3}**
1.0	**4.97922** $\times$ **10^{-2}**	**6.62989** $\times$ **10^{-2}**	**2.34706** $\times$ **10^{-2}**	**2.74331** $\times$ **10^{-2}**	**8.36988** $\times$ **10^{-3}**	**9.00613** $\times$ **10^{-3}**

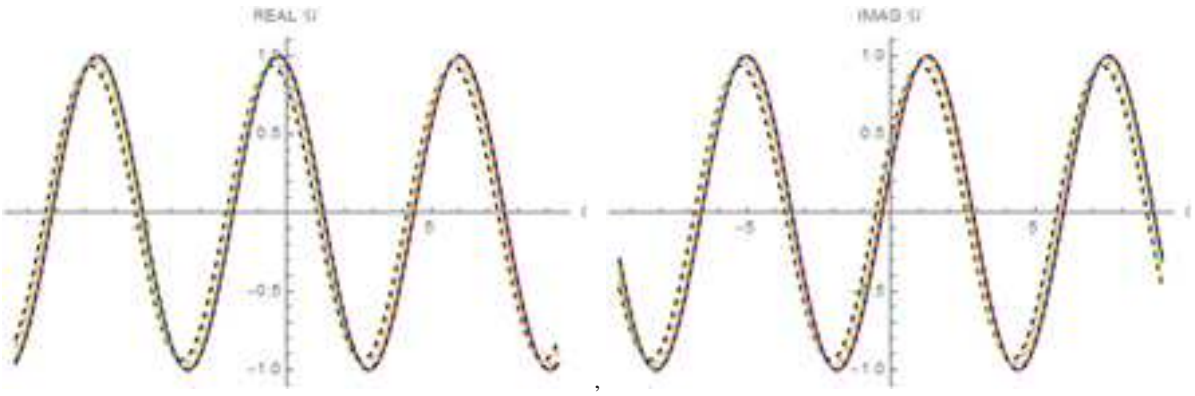

(**a**) “ (**b**)

****Exact, ****$a=1$, ****$a=0.9$, ****$a=0.8$, ****$a=0.7$, ****$a=0.6$

Fig. 1: (**a**): The 2D-Plot of the real part of $\mathscr{U}(x,t)$, against the real part of $\mathscr{U}_5(x,t)$, for Application 3, with $\psi=2,\ \phi=1, x\in[-3\pi,3\pi]$, and $t=0.3$, at distinct a values' (**b**): The 2D-Plot of the exact solution of the imaginary part of $\mathscr{U}(x,t)$, against the imaginary part of $\mathscr{U}_5(x,t)$, for Application 3, with $\psi=2,\ \phi=1, x\in[-3\pi,3\pi]$, and $t=0.3$, at distinct a values'.

Table 6. The absolute error comparison with other method for the imaginary part at various values of a for Application 4 when $t=0.1$, and $n=5$.

x_i	$\mathscr{U}_5(x,t)$	$\mathscr{U}_5(x,t)$	$\mathscr{U}_5(x,t)$	$\mathscr{U}_5(x,t)$	$\mathscr{U}_5(x,t)$	$\mathscr{U}_5(x,t)$
	a=0.7	a=0.7	a=0.8	a=0.8	a=0.9	a=0.9
	Present Method	**[60]**	**Present Method**	**[60]**	**Present Method**	**[60]**
0.1	**1.67672** $\times 10^{-2}$	**2.64768** $\times 10^{-2}$	**1.01166** $\times 10^{-2}$	**1.43136** $\times 10^{-2}$	**4.52223** $\times 10^{-3}$	**5.87486** $\times 10^{-3}$
0.2	**3.33668** $\times 10^{-2}$	**5.26891** $\times 10^{-2}$	**2.01321** $\times 10^{-2}$	**2.84842** $\times 10^{-2}$	**8.99928** $\times 10^{-3}$	**1.16910** $\times 10^{-2}$
0.3	**4.96331** $\times 10^{-2}$	**7.83749** $\times 10^{-2}$	**2.99465** $\times 10^{-2}$	**4.23702** $\times 10^{-2}$	**1.33864** $\times 10^{-2}$	**1.73904** $\times 10^{-2}$
0.4	**6.54034** $\times 10^{-2}$	**1.03278** $\times 10^{-1}$	**3.94616** $\times 10^{-2}$	**5.58328** $\times 10^{-2}$	**1.76398** $\times 10^{-2}$	**2.29159** $\times 10^{-2}$
0.5	**8.05202** $\times 10^{-2}$	**1.27148** $\times 10^{-1}$	**4.85824** $\times 10^{-2}$	**6.87376** $\times 10^{-2}$	**2.17169** $\times 10^{-2}$	**2.82126** $\times 10^{-2}$
0.6	**9.48326** $\times 10^{-2}$	**1.49749** $\times 10^{-1}$	**5.72179** $\times 10^{-2}$	**8.09555** $\times 10^{-2}$	**2.55770** $\times 10^{-2}$	**3.32273** $\times 10^{-2}$
0.7	**1.08197** $\times 10^{-1}$	**1.70853** $\times 10^{-1}$	**6.52816** $\times 10^{-2}$	**9.23646** $\times 10^{-2}$	**2.91816** $\times 10^{-2}$	**3.79100** $\times 10^{-2}$
0.8	**1.20481** $\times 10^{-1}$	**1.90250** $\times 10^{-1}$	**7.26931** $\times 10^{-2}$	**1.02851** $\times 10^{-1}$	**3.24946** $\times 10^{-2}$	**4.22140** $\times 10^{-2}$
0.9	**1.31561** $\times 10^{-1}$	**2.07746** $\times 10^{-1}$	**7.93782** $\times 10^{-2}$	**1.12309** $\times 10^{-1}$	**3.54830** $\times 10^{-2}$	**4.60961** $\times 10^{-2}$
1.0	**1.41326** $\times 10^{-1}$	**2.23167** $\times 10^{-1}$	**8.52702** $\times 10^{-2}$	**1.20646** $\times 10^{-1}$	**3.81168** $\times 10^{-2}$	**4.95177** $\times 10^{-2}$

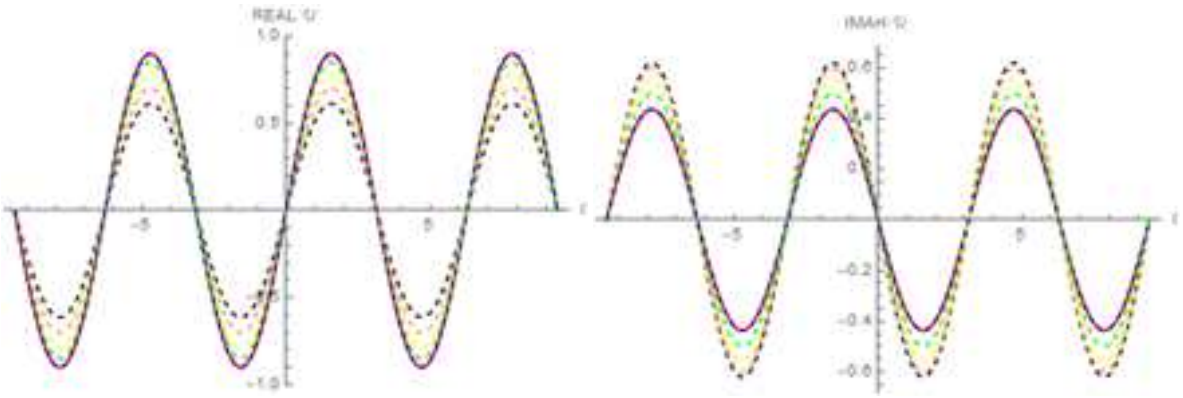

(**a**) (**b**)

$_{****}$**Exact,** $_{****}a = 1$, $_{****}$ $a = 0.9$, $_{****}a = 0.8$, $_{****}$ $a = 0.7$, $_{****}$ $a = 0.6$

Fig. 2: (a): The 2D-Plot of the real part of $\mathscr{U}(x,t)$, against the real part of $\mathscr{U}_5(x,t)$, for Application 4, with $x \in [-3\pi, 3\pi]$, and $t = 0.3$, at distinct a values', **(b)**: The 2D-Plot n of the imaginary part of $\mathscr{U}(x,t)$, against f the imaginary part of $\mathscr{U}_5(x,t)$, for Application 4, with $x \in [-3\pi, 3\pi]$, and $t = 0.3$, at distinct a values'.

6 Conclusion

This article proposes a novel iterative strategy for solving time-FSEs using the time-Caputo FD. The recommended method couples the LT with the fractional RPS scheme to generate accurate approximate and exact analytical solutions to linear and non-linear fractional models. The Laplace fractional RPS method has several advantages, including the ease of obtaining exact solutions to non-linear fractional problems, minimal calculations, depending on the limit idea, and the absence of physical parameter assumptions. The efficiency of this method is demonstrated through numerical and graphical simulation of the attained solutions, which are compared with other techniques that also use the under time-Caputo FD. From simulation view, the comparison shows that our present method provides the same exact solutions which are found via the other methods. Additionally, from 2D, and 3D-graphs the physical understanding has been illustrated with diverse FD values'. The accuracy of the future method has been highlighted in studied applications. The article concludes that the Caputo derivative is suitable for modelling time-FSEs and that the Laplace fractional RPS method is an accurate, adaptive, and efficient technique. It can also be applied to solve other types of ordinary and PDEs of non-integer order. In the future, the Laplace fractional RPS method can be used to solve more complex systems of FPDEs in various scientific fields.

Abbreviations: time-FSEs : time-fractional Schrödinger equations ; RPS :Laplace fractional residual power series; R-L : Riemann– Liouville; FD: Fractional Derivative; FPDEs: Fractional partial differential equations; LT: Laplace Transform; FPSE: fractional power series expansion; LFRE: Laplace fractional residual-error

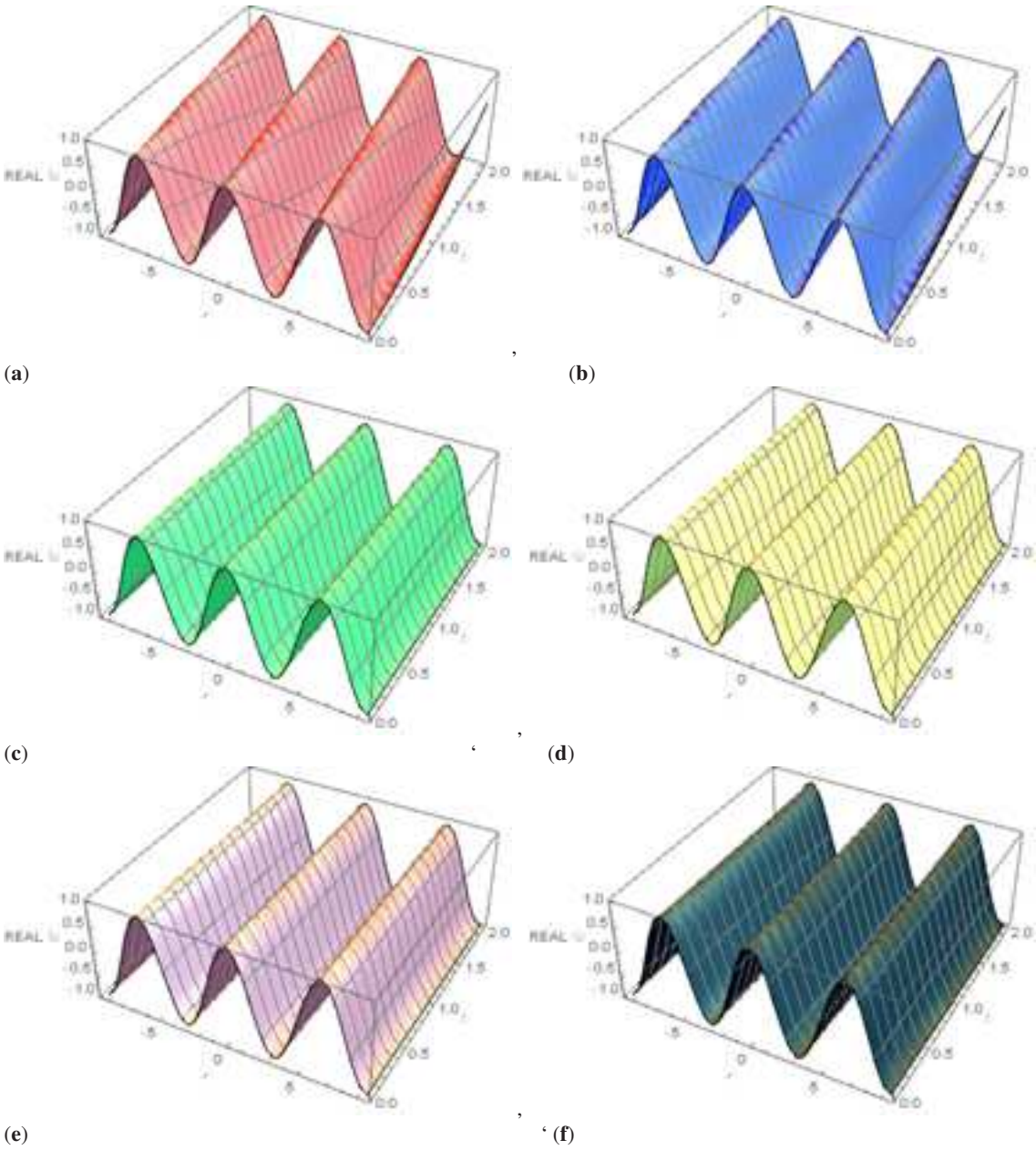

(**a**) , (**b**)

(**c**) ‘ , (**d**)

(**e**) , ‘ (**f**)

Fig. 3: 3D-Surfaces Plots of the real part of $\mathscr{U}(x,t)$, against the real part of $\mathscr{U}_5(x,t)$ for Application 3, with $\psi = 2,\ \phi = 1, t \in [0,2]$, and $x \in [-3\pi, 3\pi]$, at distinct a values' :(**a**) The real part of $\mathscr{U}(x,t)$, (**b**): The real part of $\mathscr{U}(x,t)$ at $a = 1$, (**c**): The real part of $\mathscr{U}(x,t)$ at $a = 0.9$, (**d**): The real part of $\mathscr{U}(x,t)$ at $a = 0.8$, (**e**): The real part of $\mathscr{U}(x,t)$ at $a = 0.7$, (**f**): The real part of $\mathscr{U}(x,t)$ at $a = 0.6$.

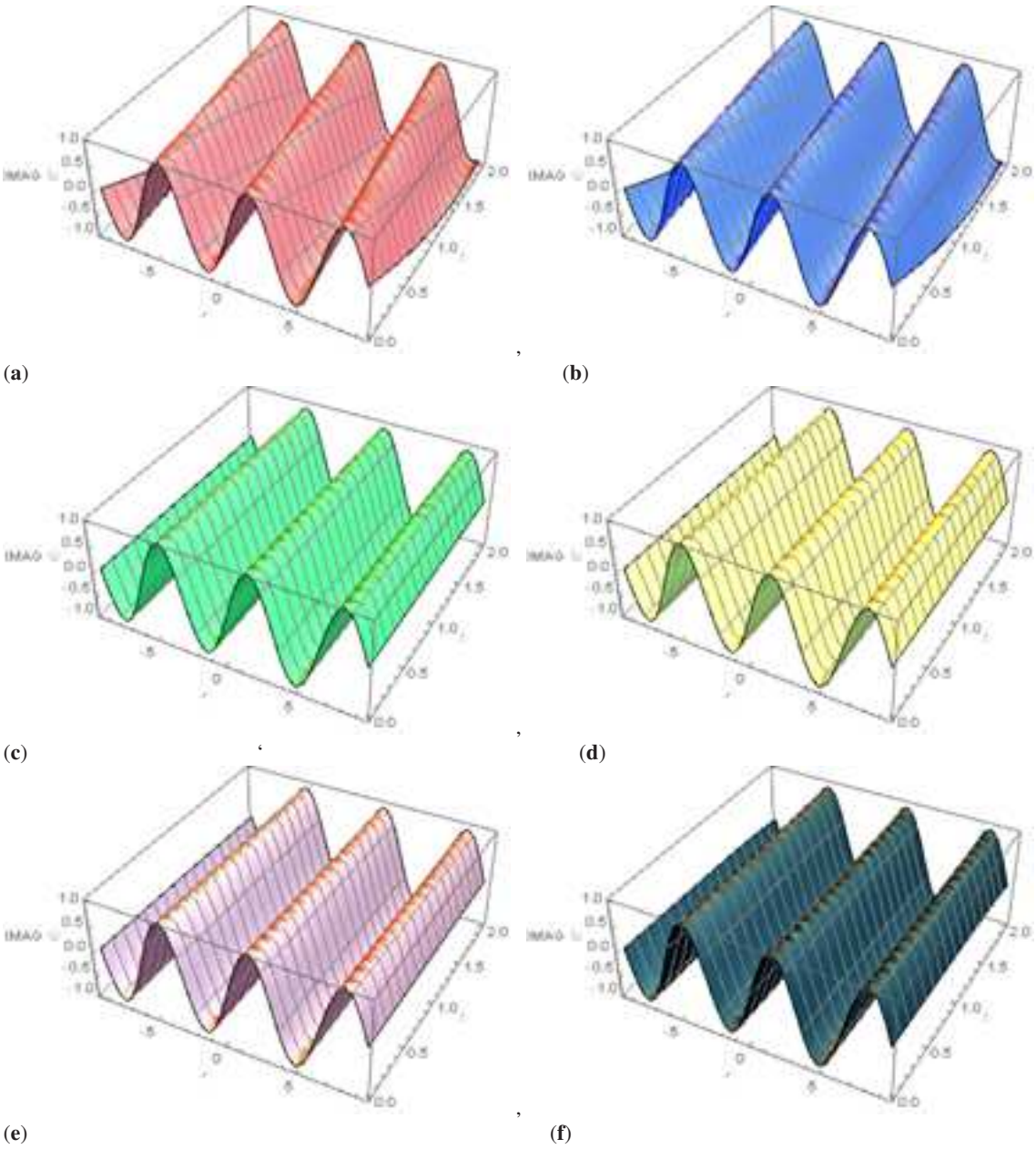

Fig. 4: 3D-Surfaces of the imaginary part of $\mathscr{U}(x,t)$, against the imaginary part of $\mathscr{U}_5(x,t)$ for Application 3, with $\psi = 2,\ \phi = 1$, $t \in [0,2]$, and $x \in [-3\pi, 3\pi]$, at distinct a values' (**a**): The imaginary part of $\mathscr{U}(x,t)$, (**b**): The imaginary part of $\mathscr{U}_5(x,t)$ at $a = 1$, (**c**): The imaginary part of $\mathscr{U}_5(x,t)$ at $a = 0.9$, (**d**): The imaginary part of $\mathscr{U}_5(x,t)$ at $a = 0.8$, (**e**): The imaginary part of $\mathscr{U}_5(x,t)$ at $a = 0.7$, (**f**): The 5imaginary part of $\mathscr{U}_5(x,t)$ at $a = 0.6$.

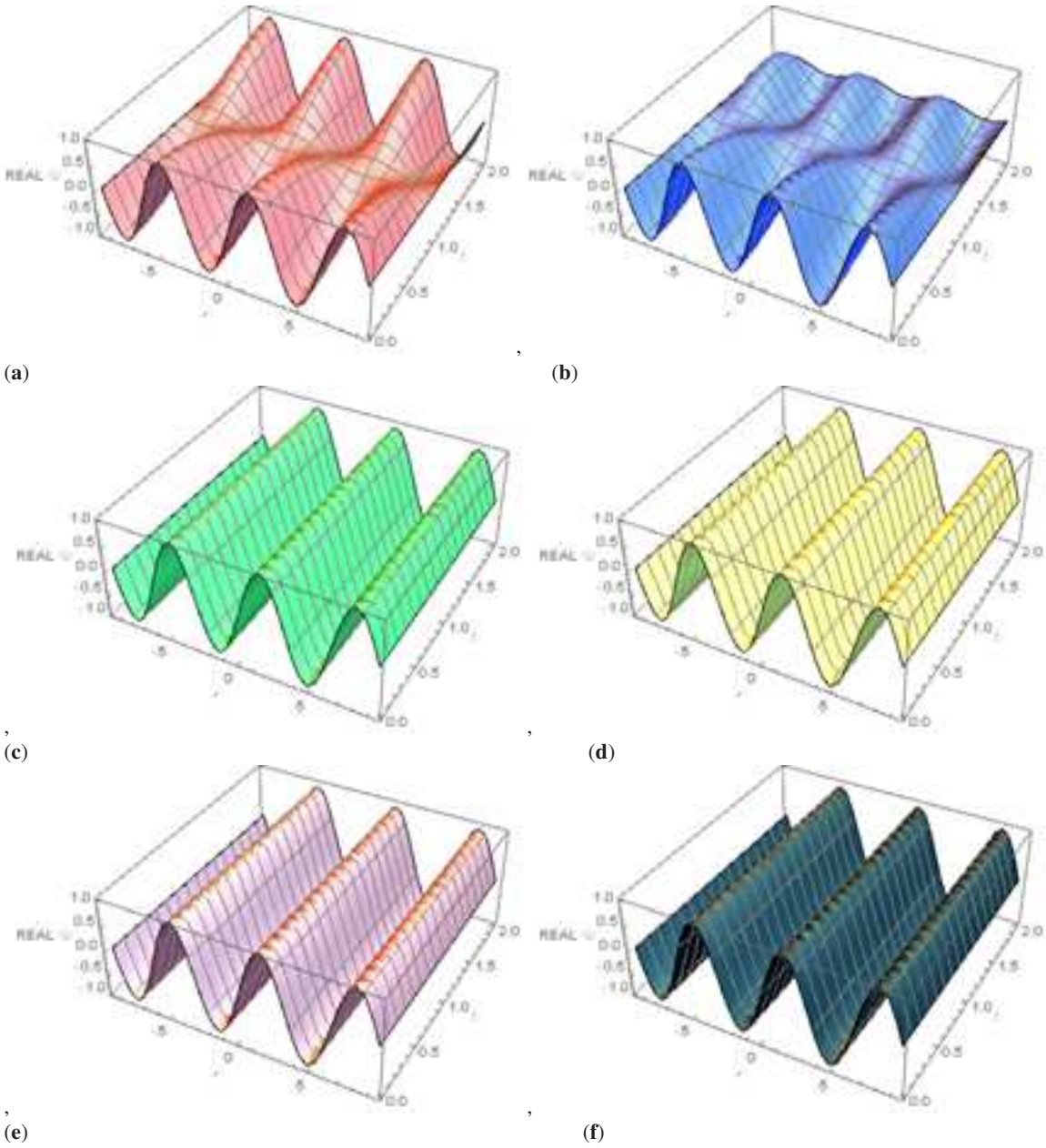

(**a**) (**b**) (**c**) (**d**) (**e**) (**f**)

Fig. 5: 3D-Surfaces Plots real part of $\mathscr{U}(x,t)$, against the real part of $\mathscr{U}_5(x,t)$ for Application 4, with $t \in [0,2]$, and $x \in [-3\pi, 3\pi]$, at distinct a values' (**a**): The real part of $\mathscr{U}(x,t)$, (**b**): The real part of $\mathscr{U}_5(x,t)$ at $a = 1$, (**c**): The real part of $\mathscr{U}_5(x,t)$ at $a = 0.9$, (**d**): The real part of $\mathscr{U}_5(x,t)$ at $a = 0.8$, (**e**): The real part of $\mathscr{U}_5(x,t)$ at $a = 0.7$, (**f**): The real part of $\mathscr{U}_5(x,t)(x,t)$ at $a = 0.6$.

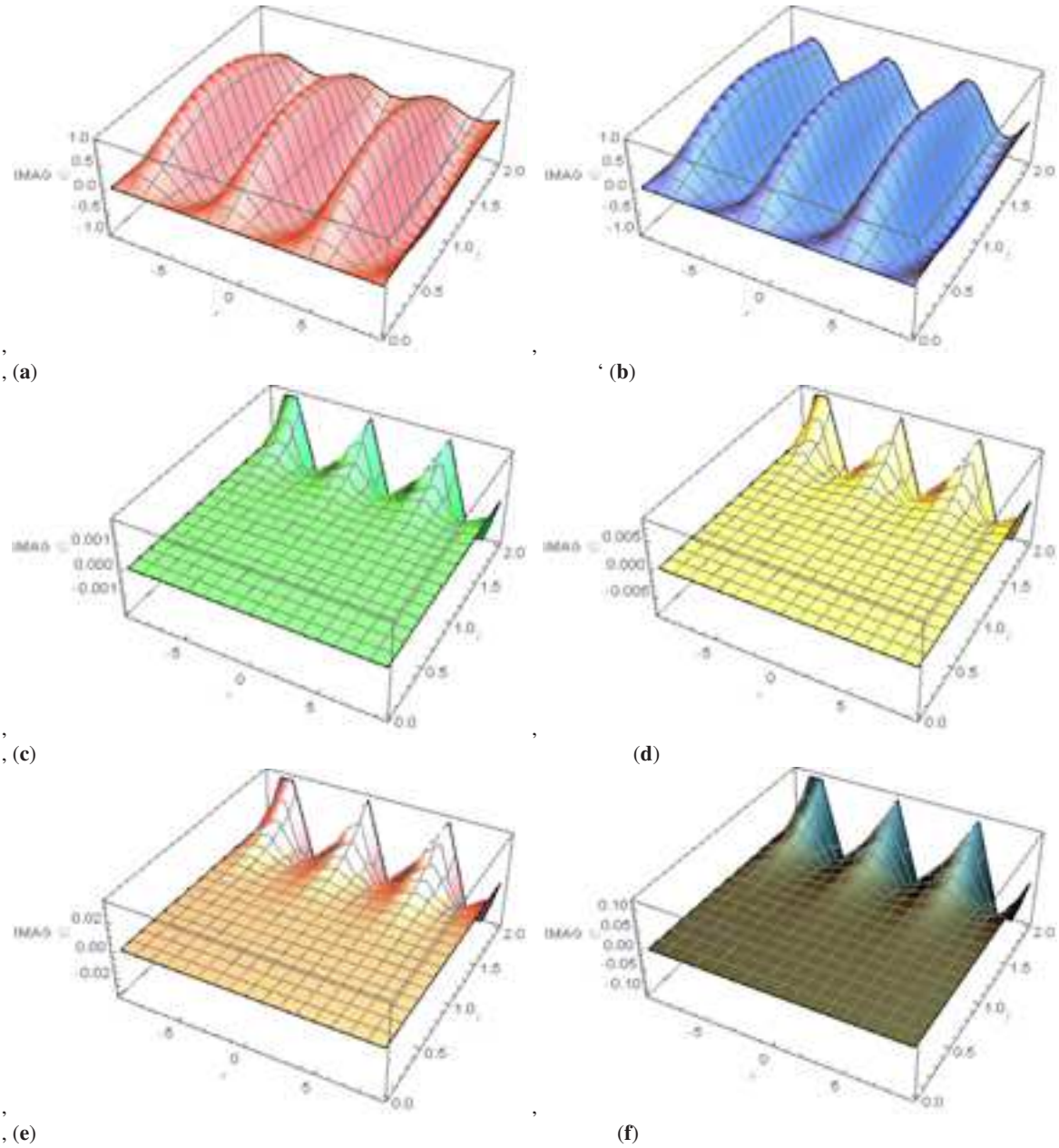

Fig. 6: 3D-Surfaces Plots of the imaginary part of $\mathscr{U}(x,t)$, against of the imaginary part of $\mathscr{U}_5(x,t)$ for Application 4, with $t \in [0,2]$, and $x \in [-3\pi, 3\pi]$, at distinct a values' (**a**): The imaginary part of $\mathscr{U}(x,t)$, (**b**): The imaginary part of $\mathscr{U}_5(x,t)$ at $a=1$, (**c**): The imaginary part of $\mathscr{U}_5(x,t)$ at $a=0.9$, (**d**): The imaginary part of $\mathscr{U}_5(x,t)$ at $a=0.8$, (**e**): The imaginary part of $\mathscr{U}_5(x,t)$ at $a=0.7$, (**f**): The imaginary part of $\mathscr{U}_5(x,t)$ at $a=0.6$

References

[1] K. B. Oldham and J. Spanier, *The fractional calculus. Integrations and differentiations of arbitrary order*, Academic Press, 1974.
[2] I. Podlubny, *Fractional differential equations*, Academic Press, 1999.
[3] F. Mainardi, M. Raberto, R. Gorenflo and E. Scalas, Fractional calculus and continuous-time finance II: The waiting-time distribution, *Phys. A* **287**, 468–481 (2000).
[4] J. H. He, Some applications of nonlinear fractional differential equations and their approximations, *Bull. Sci. Technol* **15**, 86-90 (1999).
[5] M. Al-Smadi, O. Abu Arqub and D. Zeidan, Fuzzy fractional differential equations under the Mittag-Leffler kernel differential operator of the ABC approach: Theorems and applications, *Chaos Solit. Fract.* **146**, 110891 (2021).
[6] M. Alaroud, A. K. Alomari, N. Tahal, S. Al-Omari and A. Ishak, A novel solution approach for time-fractional hyperbolic telegraph differential equation with Caputo time differentiation, *Mathematics* **11**, 2181 (2023).
[7] H. M. Srivastava, A. K. N. Alomari, K. M. Saad and W. M. Hamanah, Some dynamical models involving fractional-order derivatives with the Mittag-Leffler type kernels and their applications based upon the Legendre spectral collocation method, *Frac. Fract* **5**, 131 (2021).
[8] M. Alaroud, O. Ababneh, N. Tahat and S. Al-Omari, Analytic technique for solving temporal time-fractional gas dynamics equations with Caputo fractional derivative, *AIMS Math.* **7**, 17647-17669 (2022).
[9] N. Derdar, Nonlinear implicit Caputo-Hadamard fractional differential equation with fractional boundary conditions, *Jordan J. Math. Stat. (JJMS)*, **15**(4B), 999-1014 (2022).
[10] A. Atangana and D. Baleanu, New fractional derivatives with non-local and non-singular kernels: theory and application to heat transfer model, *Therm. Sci.* **20**, 763–769 (2016).
[11] S. Hasan, A. El-Ajou, S. Hadid, M. Al-Smadi and S. Momani, Atangana-Baleanu fractional framework of reproducing kernel technique in solving fractional population dynamics system, *Chaos Solit. Fract.* 133, 109624 (2020).
[12] M. Al-Smadi, H. Dutta, S. Hasan and S. Momani, On numerical approximation of Atangana-Baleanu-Caputo fractional integro-differential equations under uncertainty in Hilbert space, *Math. Model. Nat. Phenom.* **16**, 41 (2021).
[13] N. O. Moa'ath, A. El-Ajou, Z. Al-Zhour, R. Alkhasawneh and H. Alrabaiah, Series solutions for nonlinear time-fractional Schrödinger equations: Comparisons between conformable and Caputo derivatives, *Alexandria Engin. J.* **59**(4), 2101-2114 (2020).
[14] M. Alaroud, R. R. Ahmad and U. K. S. Din, An efficient analytical-numerical technique for handling model of fuzzy differential equations of fractional-order, *Filomat*, **33**(2), 617-632 (2019).
[15] L. Wu, L.D. Xie and J. F. Zhang, Adomian decomposition method for nonlinear differential-difference equations, *Commun. Nonlin. Sci. Numer. Simul* **14**, 12-18 (2009).
[16] M. Alaroud, M. Al-Smadi, R. R. Ahmad and U. K. S. Din, An analytical numerical method for solving fuzzy fractional Volterra integro-differential equations, *Symmetry* **11**, 205 (2019).
[17] M. Jleli, S. Kumar, R. Kumar and B. Samet, Analytical approach for time fractional wave equations in the sense of Yang-Abdel-Aty-Cattani via the homotopy perturbation transform method, *Alexandria Engin. J.* **59**, 2859–2863 (2020).
[18] M. Shqair, E. A. M. Farrag and M. Al-Smadi, Solving multi-group reflected spherical reactor system of equations using the homotopy perturbation method, *Mathematics* **10**(10):1784 (2022).
[19] D. J. Hashim, A. F. Jameel, T. Y. Ying, A. K. Alomari and N. R. Anakira, Optimal homotopy asymptotic method for solving several models of first order fuzzy fractional IVPs, *Alexandria Engin. J.* **61**(6), 4931-4943 (2022).
[20] Y. S. Daniel and S. K. Daniel, Effects of buoyancy and thermal radiation on MHD flow over a stretching porous sheet using homotopy analysis method, *Alexandria Engin. J.* **54**(3), 705-712 (2015).
[21] M. Al-Smadi, O. Abu Arqub and S. Momani, Numerical computations of coupled fractional resonant Schrödinger equations arising in quantum mechanics under conformable fractional derivative sense, *Phys. Scripta* **95**(7), 075218 (2020).
[22] M. Al-Smadi and O. Abu Arqub, Computational algorithm for solving fredholm time-fractional partial integrodifferential equations of Dirichlet functions type with error estimates". *Appl. Math. Comput* **342**, 280–294 (2019).
[23] M. Bataineh, M. Alaroud, S. Al-Omari and P. Agarwal, Series representations for uncertain fractional IVPs in the fuzzy conformable fractional sense, *Entropy* **23**(12), 1646 (2021).
[24] S. Hasan, M. Al-Smadi, A. El-Ajou, S. Momani, S. Hadid and Z. Al-Zhour, Numerical approach in the Hilbert space to solve a fuzzy Atangana-Baleanu fractional hybrid system, *Chaos Solit. Fract.* **143**, 110506 (2021).
[25] R. Nawaz, N. Ali, L. Zada, K. S. Nisar, M. R. Alharthi and W. Jamshed, Extension of natural transform method with Daftardar-Jafari polynomials for fractional order differential equations". *Alexandria Engin. J.* **60**(3), 3205-3217 (2021).
[26] G. H. Ibraheem, M. Turkyilmazoglu and M. Al-Jawary, Novel approximate solution for fractional differential equations by the optimal variational iteration method, *J. Comput. Sci.* **64**, 101841 (2022).
[27] M. Alabedalhadi, M. Al-Smadi, O. Abu Arqub, D. Baleanu and S. Momani, Structure of optical soliton solution for nonlinear resonant space-time Schrödinger equation in conformable sense with full nonlinearity term, *Phys. Scripta* **95**, 105215 (2020).
[28] M. Alaroud, N. Tahat, S. Al-Omari, D. L. Suthar and S. Gulyaz-Ozyurt,An attractive approach associated with transform functions for solving certain fractional Swift-Hohenberg equation". *J. Funct. Spac.* **2021**, 1-14 (2021).
[29] G. Arora, R. Pant, H. Emaifar and M. Khademi, Numerical solution of fractional relaxation–oscillation equation by using residual power series method, *Alexandria Engin. J.* **73**, 249-257 (2023).
[30] H, Aljarrah, M. Alaroud, A. Ishak and M. Darus, Adaptation of residual-error series algorithm to handle fractional system of partial differential equations, *Mathematics* **9**, 2868 (2021).

[31] Y. Al-Qudah, M. Alaroud, H. Qoqazeh, A. Jaradat, S. E. Alhazmi and S.Al-Omari, Approximate analytic–numeric fuzzy solutions of fuzzy fractional equations using a residual power series approach, *Symmetry* **14**, 804 (2022).
[32] M. Al-Smadi, Fractional residual series for conformable time-fractional Sawada–Kotera–Ito, Lax, and Kaup–Kupershmidt equations of seventh order, *Math. Meth. Appl. Sci.* 1-22 (2021). https://doi.org/10.1002/mma.7507.
[33] M. Al-Smadi, O. Abu Arqub and S. Hadid, Approximate solutions of nonlinear fractional Kundu-Eckhaus and coupled fractional massive Thirring equations emerging in quantum field theory using conformable residual power series method, *Phys. Scripta* **95**(10), 105205 (2021).
[34] A. El-Ajou, Adapting the Laplace transform to create solitary solutions for the nonlinear time-fractional dispersive PDEs via a new approach, *Europ. Phys. J. Plus* **136**(2), 229 (2021).
[35] J. Hanna and J. Rowland, *Fourier series, transforms and boundary value problems*, Wiley, New York, 1990.
[36] H. Aljarrah, M. Alaroud, A. Ishak and M. Darus, Approximate solution of nonlinear time-fractional PDEs by Laplace residual power series method, *Mathematics* **10**(12), 1980 (2022)
[37] M. Alaroud, Application of Laplace residual power series method for approximate solutions of fractional IVP's, *Alexandria Engin. J.* **61**(2), 1585-1595 (2021).
[38] H. Aljarrah, M. Alaroud, A. Ishak and M. Darus, A novel analytical LRPSM for solving nonlinear systems of FPDEs, *Fract. Fract.* **6**(11), 650 (2022).
[39] H. Aljarrah, M. Alaroud, A. Ishak, M. Darus and S. Momani, Exact and approximate solutions of heat fractional differential equation using Laplace residual power series method. *International Conference on Fractional Differentiation and Its Applications (ICFDA)*, Ajman, United Arab Emirates, **2023**, pp. 1-5.
[40] M. Alaroud, A. K. Alomari, N. Tahat and A. Ishak, Analytical computational scheme for multivariate nonlinear time-fractional generalized biological population model, *Frac. Fract.* **7**(2), 176 (2023).
[41] N. Laskin, Fractional quantum mechanics and Lévy path integrals, *Physics Lett. A* **268**(4-6), 298-305 (2000).
[42] N. Laskin, Fractional quantum mechanics, *Phys. Rev. E* **62**(3), 3135 (2000).
[43] N. Laskin, Fractional Schrödinger equation, *Phys. Rev. E* , **66**(5), 056108 (2002).
[44] F. Bardou, J. P. Bouchaud, O. Emile, A. Aspect and C. Cohen-Tannoudji, Subrecoil laser cooling and Lévy flights, *Phys. Rev. lett.* **72**(2), 203 (1994).
[45] B. Saubaméa, M. Leduc and C. Cohen-Tannoudji, Experimental investigation of nonergodic effects in subrecoil laser cooling, *Phys. Rev. lett.* **83**(19), 3796 (1999).
[46] S. Schaufler, W. P. Schleich and V. P. Yakovlev, Keyhole look at Levy flights in subrecoil laser cooling *Phys. Rev. lett.* 83(16), 3162 (1999).
[47] H. Katori, S. Schlipf and H. Walther, Anomalous dynamics of a single ion in an optical lattice, *Phys. Rev. Lett.* **79**(12), 2221 (1997).
[48] N. Mercadier, W. Guerin, M. Chevrollier and R. Kaiser, Lévy flights of photons in hot atomic vapours, *Nature Phys.* **5**(8, 602-605 (2009).
[49] J. Klafter, A. Blumen and M. F. Shlesinger, Stochastic pathway to anomalous diffusion, *Phys. Rev. A* **35**(7), 3081 (1989).
[50] G. M. Zaslavsky, Fractional kinetic equation for Hamiltonian chaos, *Physica D* **76**(1-3), 110-122 (1994).
[51] A. I. Saichev and G. M. Zaslavsky, Fractional kinetic equations: solutions and applications, *Chaos* **7**(4), 753-764 (1997).
[52] G. Zimbardo, P. Veltri, G. Basile and S. Principato, Anomalous diffusion and Lévy random walk of magnetic field lines in three dimensional turbulence, *Phys. Plas.* 2(7), 2653-2663 (1995).
[53] A. K. Mittal and L. K. Balyan, Numerical solutions of two-dimensional fractional Schrodinger equation, *Math. Sci.* **14**(2), 129-136 (2022).
[54] M. T. Islam, M. A. Akbar, J. F. Gómez-Aguilar, E. Bonyah and G. Fernandez-Anaya, Assorted soliton structures of solutions for fractional nonlinear Schrodinger types evolution equations,*J. Ocean Engin.Sci.* **7**(6), 528-535 (2022).
[55] M. T. Islam, M. A. Aktar, J. F. Gómez-Aguilar and J. Torres-Jiménez, Further innovative optical solitons of fractional nonlinear quadratic-cubic Schrödinger equation via two techniques, *Opt. Quant. Electr.* **53**, 1-19 (2021.
[56] H. Yépez-Martínez, H. Rezazadeh, J. F. Gómez-Aguilar and M. Inc, A new local fractional derivative applied to the analytical solutions for the nonlinear Schrödinger equation with third-order dispersion, *J. Nonlin. Opt. Phys. Mat.* **31**(3), 2250011 (2022).
[57] M. T. Islam, M.A. Akter, J. F. Gómez-Aguilar and M. A. Akbar, Novel and diverse soliton constructions for nonlinear space–time fractional modified Camassa–Holm equation and Schrodinger equation, *Optical Quant. Electr.* **54**(4), 227 (2022).
[58] S. R. Aderyani, R. Saadati, J. Vahidi and J. F. Gómez-Aguilar, The exact solutions of conformable time-fractional modified nonlinear Schrödinger equation by first integral method and functional variable method, *Optical Quant. Electr.* **54**(4), 218 (2022).
[59] I. G. Ameen, R. O. A. Taie and H. M. Ali, Two effective methods for solving nonlinear coupled time-fractional Schrödinger equations, *Alexandria Engin. J.* **70**, 331-347 (2023).
[60] M. I. Liaqat and A. Akgül, A novel approach for solving linear and nonlinear time-fractional Schrödinginger equation, *Chaos Solit. Fract.* **162**, 112487 (2022).
[61] Y. Zhang, A. Kumar, S. Kumar, D. Baleanu and X. J. Yang, Residual power series method for time-fractional Schrödinger equations, *J. Nonlin. Sci. Appl.* **9**(11), 5821-5829 (2016).
[62] A. Borhanifar and R. Abazari, Numerical study of nonlinear Schrödinger and coupled Schrödinger equations by differential transformation method, *Optics Commun.* **283**(10), 2026-2031 (2010).
[63] H. Wang, Numerical studies on the split-step finite difference method for nonlinear Schrödinger equations, *Appl. Math. Comput.* **170**(1), 17-35 (2005).

[64] N. A. Khan, M. Jamil and A. Ara, Approximate solutions to time-fractional Schrödinger equation via homotopy analysis method, *Int. Sch. Res. Not.* **2012**, 2012, doi:10.5402/2012/197068.
[65] A. Sadighi and D. D. Ganji, Analytic treatment of linear and nonlinear Schrödinger equations: a study with homotopy-perturbation and Adomian decomposition methods, *Phys. Lett. A* **372**(4), 465-469 (2008).
[66] A. R. Kanth and K. Aruna, Two-dimensional differential transform method for solving linear and non-linear Schrödinger equations, *Chaos Solit. Fract.* **41**(5), 2277-2281 (2009).
[67] A. M. Wazwaz, A study on linear and nonlinear Schrodinger equations by the variational iteration method, *Chaos Solit. Fract.* **37**(4), 1136-1142 (2008).